AN ADAPTIVE NEURO-FUZZY APPROACH FOR MODELING THE EFFECTS OF WATER-IN-DIESEL EMULSION ON DIESEL SPRAYS

A Thesis Submitted to
the Graduate School of Engineering and Sciences of
İzmir Institute of Technology
in Partial Fulfilment of the Requirements for the Degree of

MASTER OF SCIENCE

in Energy Engineering

by
Bekir Kağan YAVUZ

September 2016
İZMİR

We approve the thesis of **Bekir Kağan YAVUZ**

Examining Committee Members:

_____
Asst. Prof. Dr. Ünver ÖZKOL
Department of Mechanical Engineering
İzmir Institute of Technology

_____
Asst. Prof. Dr. Turhan ÇOBAN
Department of Mechanical Engineering
Ege University

_____
Asst. Prof. Dr. Alvaro DIEZ
Department of Mechanical Engineering
İzmir Institute of Technology

22 September 2016

_____
Asst. Prof. Dr. Alvaro DIEZ
Supervisor
Department of Mechanical Engineering
Izmir Institute of Technology

_____
Asst. Prof. Dr. Kemal SAPLIOĞLU
Co-Supervisor
Department of Civil Engineering
Suleyman Demirel University

_____
Prof. Dr. Gülden Gökçen AKKURT
Head of the Department of Energy Engineering

_____
Prof. Dr. Aysun SOFUOĞLU
Dean of the Graduate School of Engineering and Science

ACKNOWLEDGMENTS

I would like to express my gratitude and sincere thanks to my supervisor Alvaro Diez for the vital comments, remarks and engagement through the learning process of this master thesis. I would like to thank also my co-supervisor Kemal Saplıoğlu for his supports especially in methodology.

Many thanks also go to IZTECH for converting my time into a great experience during my Master of Science period.

I am also grateful to my parents, my wife and my sister for the unceasing encouragement and I would like to thank my loved ones, who have supported me throughout entire process, both by keeping me harmonious and helping me putting pieces together. I will be grateful forever for their love.

ABSTRACT

AN ADAPTIVE NEURO-FUZZY MODELING OF THE EFFECTS OF WATER-IN-DIESEL EMULSION ON DIESEL SPRAYS

This thesis is prepared as an outcome of the Energy Engineering Master of Science program at Izmir Institute of Technology, IZTECH, in Turkey. The main purpose of this study is to analyse the effects of water content in diesel fuel spray behaviours using adaptive neuro-fuzzy inference system models (ANFIS) for compression ignition engines.

The investigations are carried out using numerical models of ANFIS in MATLAB R2011a, generating simulations from training and test datasets based on recent experimental studies from the literature. The thesis primarily tests the use and the fitness of ANFIS models, modifying the neural network structure so that the simulations acceptably reach the experimental results accurately. Then secondarily, the simulation is used to investigate the effects of parameters originally not available in the related study.

The investigation mainly focusses on water in diesel emulsions from pure diesel to an emulsion with 20% water content. Operational conditions such as chamber ambient pressure, injection pressure, chamber ambient temperature are also investigated to find their effects over spray penetration.

It was found that the increase of water content in the diesel fuel did not have a relevant effect at very low and very high temperatures, however at medium-high temperatures it increased spray penetration. Furthermore, it was observed that the increase of chamber ambient pressure and chamber ambient temperature reduced the spray penetration as expected.

ÖZET

SU İÇEREN DİZEL EMÜLSİYONLARININ DİZEL SPREYLER ÜZERİNDEKİ ETKİSİNİN UYARLANIR SİNİRSEL BULANIK MANTIK İLE MODELLENMESİ

Bu çalışma İzmir Yüksek Teknoloji Enstitüsü, Enerji Mühendisliği Yüksek Lisans programının bitirme tezidir.

Tezin ana amacı su içeren dizel emülsiyonlarının dizel spreyler üzerindeki etkisinin uyarlanır sinirsel bulanık mantık (ANFIS) ile modellenerek incelenmesidir.

Çalışmalar literatürdeki güncel deneysel çalışmalardan baz alınan bilgilerin MATLAB R2011a yazılımı üzerinden ANFIS modellere eğitim ve test datası olarak aktarılmasıyla gerçekleştirilmiştir. Tez öncelikle ANFIS modeli kullanılabilirliğini ve doğruluğunu incelemektedir. Buna ulaşırken ANFIS modellerin girdi yapıları modifiye edilmiştir böylece simülasyonun deneysel sonuçlara göre yeterli doğrulukta sonuçlar vermesi sağlanmıştır. Sonrasında ANFIS model ilgili literatür çalışmalarında mevcut bulunmayan bir parametrenin sonuçlar üzerindeki etkisinin incelenmesi amacıyla kullanılmıştır.

Çalışmalar genel olarak su içeren dizel emülsiyonlar üzerine yapılmıştır. Saf dizelden %20 su katkılı dizele kadar olan yakıtlar incelenmiştir. Ayrıca silindir ortam basıncı, enjeksiyon basıncı ve silindir ortam sıcaklığı gibi farklı operasyonel koşulların sprey penetrasyonu üzerine etkileri de incelenmiştir.

Çalışmalar sonucunda dizel yakıt içindeki su içeriğinin artmasının, enjeksiyon basıncına benzer şekilde, sprey penetrasyonunu olumlu etkilediği görülmüştür. Diğer taraftan, silindir ortam basıncı ve silindir ortam sıcaklığının penetrasyon miktarını olumsuz etkilediği gözlemlenmiştir.

LIST OF CONTENTS

LIST OF FIGURES

Figure **Page**

LIST OF TABLES

LIST OF SYMBOLS

Symbols

A	Area	m^2
B	Bore	m
C	Heat Capacity	J/K
c_p	Specific heat at Constant Pressure	J /kg K
D_h	Hydraulic Diameter	M
E	Energy	J
F/A	Fuel-Air-Ratio	-
h_g	Heat Transfer Coefficient	W/m^2K
H	Enthalpy	J
M	Molar Mass	kg /kmole
m	Mass	kg
N	Crankshaft Rotational Speed	rev/s
Q_{loss}	Heat Loss	J
p	Pressure	Pa
R	Universal Gas Constant	J/K mol
t	Time	s
T	Temperature	K
W	Work	J
U	Heat Transfer	J
V	Cylinder Volume	m^3
λ	Air-fuel Equivalence Ratio	-
ρ	Density	kg/m^3
η	Efficiency of Engine	-
γ	Specific Heat Ratio	-
θ	Crank angle	Degree

LIST OF ABBREVIATIONS

ANFIS:	Adaptive Neuro-Fuzzy Inference System
ANN:	Artificial Neural Network
ASOI:	After Start of Injection
BDC:	Bottom Dead Center
BMEP:	Break Mean Efficiency Pressure
BSOI:	Before Start of Injection
CAD:	Crank Angle Degree
CFD:	Computational Fluid Dynamics
CID:	Combustion Initiation Duration
COV:	Coefficient of Variation
DI:	Direct Injection
EVC:	Exhaust Valve Closing
D:	Pure Diesel
D10	10% Water and 90% Diesel
D20:	20% Water and 80% Diesel
EGR:	Exhaust Gas Recirculation
FIS:	Fuzzy Inference System
FL:	Fuzzy Logic
FTDC:	Fire Top Dead Center, (TDC close to spark timing)
GDI:	Gasoline Direct Injection Engine
GE:	Gas Exchange
HC:	Hydrocarbons
HCCI:	Homogeneous Charge Compression Ignition
HRR:	Heat Release Rate
IMEP:	Indicated Mean Effective Pressure
IVC:	Intake Valve Closing
IVO:	Intake Valve Opening
LHV:	Lower Heating Value
MBT:	Minimum Advance for Best Torque
MFB:	Mass Fraction Burned
PFI:	Port Fuel Injection

RPM:	Revolutions Per Minute
Rc:	Compression Ratio
SIDI:	Spark Ignition Direct Injection Engine
SoC:	Start of Combustion
SoI:	Start of Injection
ST:	Spark Timing
SI:	Spark Ignition
TDC:	Top Dead Center
WiDE:	Water in Diesel Emulsion

CHAPTER 1

INTRODUCTION

1.1. Thesis' Aim and Objectives

Nowadays, the effects of the vehicles on air pollution have been remarkably increasing day after day with increasing number of vehicles. The emissions regulations are getting more stringent annually which spread all around the world. Moreover, continuously increasing price of the fuel is forcing the industry to produce more efficient engines. Under these circumstances, the basic challenges in automotive industry are as follows:

- Higher power output
- Lower specific fuel consumption
- Lower emission values
- Lower noise
- More comfortable driving

The emission of combustion products into the atmosphere has been recently discussed seriously along with the use of the internal combustion engines. The regulations of national and regional authorities all around the world as well as the global agreements have become more stringent. The comprehension and the concerns about global pollution have been remarkably increased (Mohan et al., 2013). The emissions of soot, particular matter (PM) and nitrogen oxides (NO_X) are concerned in particular (Namasivayam et al., 2010).

The engines' emissions and specific fuel consumption are obviously related with the engine performance and this is closely related to the fuel and air mixture within the cylinder. Thus the understanding of the spray behaviour in the combustion chamber is so essential. The spray penetration after the fuel injection is one of the main parameter in terms of spray behaviour of an internal combustion engine.

This study focuses on the effects of water additive through emulsifiers which forms water-in-diesel emulsions on spray penetration. Such emulsions have pointed the potential to improve the spray behaviours of a compression ignition (CI) engine. This can be defined by the enhanced air fuel mixing process presented by improved atomization since microexplosions may take place due to the remarkable volatility difference between the different phases of the fuel. Moreover, water disassociation can form hydroxyl radicals during combustion which assist to oxidize the soot that being so decreasing soot emissions (Huo et al., 2014).

1.2. Organization of Thesis

The structure of the thesis can be summarized as follows:

In Chapter 2, a literature survey is presented where studies on diesel sprays, studies on Artificial Neural Network (ANN) on Compression Ignition (CI) engines and studies on Adaptive Neuro-Fuzzy Inference System (ANFIS) on CI engines are examined. The studies on diesel sprays cover theoretical, experimental and numerical Computational Fluid Dynamics (CFD) studies.

The studies on ANN and ANFIS related to internal combustion engines in the literature are tabulated and compared in terms of their models' accuracy and error values. These investigations guide this thesis during the modelling especially on the inputting of the data to reach more accurate results.

In Chapter 3, the water in diesel emulsion is explained in detail. The properties and effects of emulsions over fuels are examined. Then an ANFIS numerical approach is used in MATLAB to analyse the effects of emulsions. Finally, the performance criteria of tools are technically determined.

In Chapter 4, the data collected from the experimental results available in the literature are explained. They are two recent experimental studies, in which this ANFIS approach is carried out. The data are tabulated dividing as training and test dataset and used in the ANFIS simulation. Afterwards, the combination of dataset of these separate studies is simulated at the same time to understand the effects of parameters which are originally not available in one of these studies.

In Chapter 5, a full discussion of the results is presented. The training dataset is inputted and test dataset is used to control the software. The inspection of the software is

firstly disclosed. Then the results are shown calculating their accuracy with performance criteria.

In the final chapter, Chapter 6, the methodology and results are simply explained. The advantages and drawbacks are then summarized as well as the conclusion on thesis's results of spray penetration.

CHAPTER 2

LITERATURE SURVEY

2.1. Studies on Diesel Spray

Spray and combustion characteristics of fuels under a different range of conditions have been investigated and developed in recent years due to the increasing stringent emission regulations as well as the depletion of fossil fuels. The characterization of many parameters related to specific spray features such as tip penetration, spreading angle, liquid phase penetration etc. raised an important step forward in the understanding of the injection phenomena (Naber & Sieber, 1996; Roisman et al., 2007; Payri et al., 2014).

In diesel engines, spray penetration is usually changed by the in-cylinder gas flow. Accurate prediction of diesel spray with gas flow is important to the optimal design of diesel fuel injection system in order to increase the efficiency and reduce emissions (Xu et al., 2016).

2.1.1. Theoretical Studies on Diesel Spray

The spray development initiates with the liquid fuel being injected in an ambient at high pressure and a certain temperature. Once the fuel is injected into the cylinder, the fuel spray penetrates along the axis and entrains the surrounding air. Because of consequently small temporal and spatial scales resulted from the high velocity spray, the diesel spray evolution is an intrinsically complicated problem (Xu et al., 2016). Also, it is hard to predict spray parameters accurately.

In the past decades, semi-empirical formulas based on experimental data have been thoroughly used to forecast the penetration of the diesel sprays. Dent (1971) and Hay & Jones (1972) resolved that the penetration distance is proportional to the square root of time from experiment results from their spray experimental results. A more detailed analysis was developed that the penetration distance is proportional to the initial short time (jet break-up time) (Lefebvre, 1989; Borman & Ragland, 1998).

Reitz and Yoshizaki (1986) took the spray process as two stages, before and after break-up time, and gave distinctive formulas for the penetration of the two stages.

Some studies took the in-cylinder gas flow into consideration in spray experiments, and provided correlations that account for in cylinder gas flow (Hiroyasu et al., 1980; Sinnamon et al., 1980; Takasu et al., 2013).

Additionally, Naber (1996) and Desantes et al. (2006) aroused more detailed theoretical models out of the momentum flux conservation along the spray axis in order to predict spray penetration. Sazhin (2001) originated a model for fuel spray penetration from two-phase theory. Pastor et al. (2008) provided a research focusing on the transient formation of diesel sprays and derived a 1D model for the representation of mixing-controlled inert diesel sprays. In that study, the increase in flame radial width and decrease in local density are found as governing the diesel flame development.

Xu et al. (2016) has recently demonstrated a theory concentrating on the penetration of diesel spray with gas flow. In order to perceive the effect of gas flow on the penetration of diesel spray, a one-dimensional spray model was developed from an idealized diesel spray, which is able to predict the spray behaviour under various gas flow conditions. The principles of conservation of mass and momentum were used in the derivation of idealizing the spray model with only axial gas flow as shown in Figure 2.1. Momentum of in-cylinder air flow was also taken into consideration. Proof of the model at stable condition was accomplished by comparing model forecasts with experimental measurements of diesel spray without gas flow from Naber's experiments (1996). Additionally, CFD simulations on penetration of diesel spray with gas flow were performed with the commercial code of AVL Fire. The one-dimensional model was corroborated by the penetration results with gas flow from CFD computations. Results of the paper displayed that a reasonable approximation of the spray development could be obtained for both with and without ambient gas flow conditions.

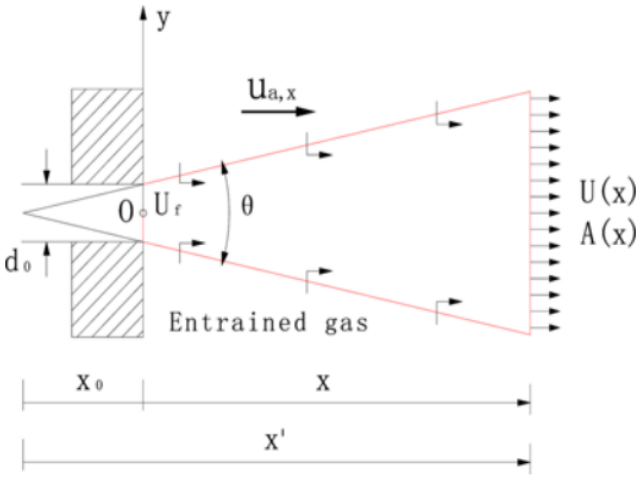

Figure 2.1. Schematic of the idealized spray model with only x-axial gas flow (Source: Xu et al., 2016)

The representational figure above shows the spray model where d_o is the orifice diameter, or nozzle hole; x is the distance along axial direction; U is the velocity vector of spray; θ is full cone angle of the real spray and A is the cross sectional area. Also, a control surface (red line in Figure 2.1) is specified in the idealized spray model, and utilized for the mass and momentum balances.

2.1.2. Experimental Studies on Diesel Spray

Spray behaviours including spray penetration which are investigated experimentally are widely found in the literature. The most common methodology among the researches is that the investigations in optically accessible chambers using various types of high-speed camera configurations. The image files produced during experiments are then processed. After image processing tools the figures are structured to reach results and to complete study. The focus of these investigations includes atomization of emulsion spray as well as regular diesel spray.

The definition and experimental characterization of many parameters related to specific spray features such as tip penetration, spreading angle, liquid phase penetration, lift-off length etc. brought an important step forward in the apprehension of the process (Naber & Sieber, 1996; Payri et al., 2014). Consequently, conceptual and numerical models have been developed to simulate the whole diesel injection process defining the

complex physical and chemical processes that occur behind the experimental examination (Kiplimo et al., 2012; Musculus & Kattke, 2009). In all likelihood, the most important contributions in this direction are two conceptual models for conventional combustion and low temperature combustion based on different optical techniques proposed by Dec (1997) and Musculus (2013), which give detailed enhancement about how fuel-air mix in reacting conditions.

The increasing need for more accurate and predictive models together with the possibility of performing more detailed experiments still highlight some lack of knowledge. Few studies in the literature address the effect that combustion has on the shape and mixing of the spray. Siebers's study (2009) showed that the reacting spray evolution depends on the ambient density of the cylinder. The similar trend was also observed by Pickett and Hoogterp (2009). The spray penetration under reacting conditions was studied by Desantes et al. (2014) and one outlined spreading angle was applied for asserting the radius of expansion. In Pickett's study (2009), the reacting and non-reacting spray penetration were also investigated with the high speed "Schlieren" imaging technique. The Schlieren imaging technique allows to uncover gradients in the refractive index of a transparent medium (Benajes et al., 2013). The technique depends on the deviation of a light beam developed when light transits heterogeneous fluids.

Atomized emulsion sprays were demonstrated in separate experiments by a number of investigators especially in terms of micro explosions. For the non-combusting spray, Mattiello et al. (1992) studied the water and fuel oil emulsion flames by laser light scattering. The scattered light concentration analysis of the polarization ratio revealed the incidence of micro-explosion in the flame. Wu et al. (2007) used laser holograph shawdography to visualize the spray in a diesel and water and ethanol emulsion in which a part could be seen in the main jet body which suggested the occurrence of micro-explosions. Watanabe and Okazaki (2013) used high speed imaging to visualize the secondary atomization in an emulsified fuel spray flow by shadow imaging; they reported puffing and partial-micro-explosions, but complete micro-explosions were rarely observed. For the combusting spray, the direct flame photographs, temperature profiles and micro explosion frequencies have been shown by Fuchihata et al. (2003) in which they reported observation of small droplets with diameters less than 50 μm exploding in the spray flame. In the study of Raul et al. (2010), some ‘‘glowing spots’’ were detected inside the burning spray and might have resulted from micro-explosion.

Huo et al. (2014) investigated the initial liquid penetration in addition to some other combustion characteristics. They have shown that emulsified fuel remains a potential solution to meet the increasingly stringent emission legislations for internal combustion engines due to its capability of simultaneously reducing NO_X and particular matter (PM). Emulsified diesels with 10% and 20% water by volume were studied and the stability of the water emulsified diesel was first investigated in terms of the hydrophilic-lipophilic-balance (HLB) value in that research. High speed imaging with a pulse duration of 25 ns was used to capture the spray and combustion process under various conditions. Results of that study showed that longer initial liquid penetration for emulsified diesel under low ambient temperatures and also longer ignition delay of emulsified diesel provided more air/fuel mixing time, thus significantly lowering the soot luminosity.

Payri et al. (2015) studied the shape of diesel spray at actual engine conditions in a constant pressure flow facility (CPF). The Schlieren imaging technique was used to carry out quantitative measurements of spray tip penetration and radial width, as shown in Figure 2.2. Experimental layout: the test chamber is presented together with the optical setup. The effects of different operating parameters such as injection pressure, ambient temperature, ambient density, and O_2 concentration, on the axial and radial expansion were also investigated. Based on those results, the reacting spray could be divided into three parts: an inert part, a transient one, and a quasi-steady one that lies between the two other regions. Results demonstrated that the radial expansion rises with increasing injection pressure and decreasing ambient temperature and ambient density. The oxygen concentration did not have any obvious effect on the radial expansion.

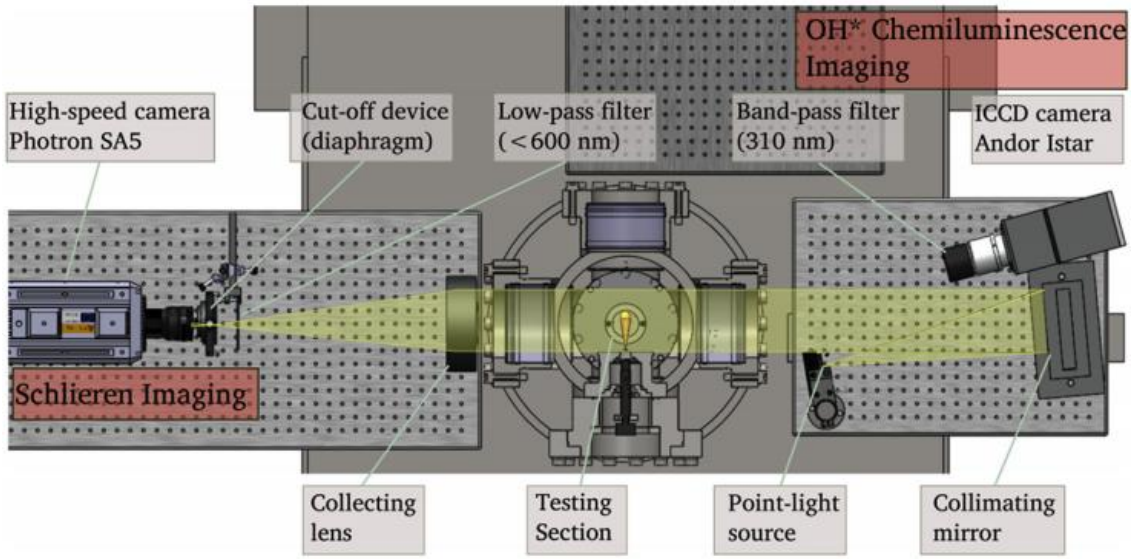

Figure 2.2. Experimental layout: the test chamber is presented together with the optical setup (Source: Payri et al., 2015)

Palani et al. (2015) investigated that the combustion and emission characteristics of inedible oils and their derivatives were quite different from those of mineral diesel; in particular, inedible oils and their derivatives present higher molecular, relative density, and vaporization characteristics. The spray properties of fuel mainly depended on the fuel injection pressure, density, viscosity, ambient pressure, and temperature. Among those parameters, fuel injection pressure more importantly affected the spray structure. In that study, experiments were carried on using diesel, jatropha oil methyl-ester, karanja oil methyl-ester, and two other biodiesel blended fuels (JB20 and KB20; in which the number was indicating the volumetric ratio of the biodiesel) in a diesel engine with different injection pressures. Macroscopic spray properties, such as spray tip penetration, spray cone angle, and spray area, were acquired from images captured by a high-speed video camera. The sauter mean diameter and spray volume of all of the tested fuels were also estimated. Experimental results showed that the biodiesel blends demonstrate features different from those of diesel fuel. KB100 presented the highest spray tip penetration and spray area, followed by JB100 JB20, KB20 and diesel. Diesel fuel showed the best spray parameters in terms of spray cone angle (degree) and spray area (cm^2) which was followed by JB20, KB20, KB100 and JB100. The tested fuels exhibited better spray characteristics at higher injection pressures to the lower ones.

Emberson et al. (2016) studied on Diesel fuel and water emulsions which have been shown to reduce emissions of NO_X and PM from compression ignition engines.

They determined that there is a lack of work examining the influence of emulsification on the sprays formed during injection. Their work investigated the spray cone angle and tip penetration of Diesel fuel and water emulsions, containing 10% and 20% water (by mass). All experiments were conducted under non-reacting, non-vaporizing conditions in a constant volume pressure chamber filled with nitrogen. A focused shadowgraph system, with high speed photography, coupled with a research, high current LED system was used. Differences in the spray cone angles presented that the emulsification had an effect for the injections at a pressure of 500 bar. Emulsification did not have any perceptible effect on the spray tip penetration. Spray tip penetration displayed agreement with previous trends in terms of proportionality to time after start of injection however agreement with models found from the literature was not consistent.

2.1.3. CFD Studies on Diesel Spray

Improvement of the performance of a direct injection diesel engine requires various multiple injection strategies and increased engine compression ratio. Lee et al. (2011) explored the properties of spray tip penetration with 0-D and 3-D CFD simulations over a wide range of ambient gas densities. They created a 0-D simulation of the experimental outputs of Naver and Siebers (1996) and Desantes et al. (2015) based on Abani and Reitz's (2007) concept of an effective injection velocity. Moreover, CFD simulation was carried on for various gas jet models which introduced various gas jet velocity distributions. Lee and Reitz (2012) compared CFD simulations of the spray tip penetration with their own gas jet models and the KIVA-3V standard model which is a Fortran based Computational Fluid Dynamics software developed by Los Alamos National Laboratory (Amsden, 1997). Spray tip penetrations as a function of both changes in the compression ratio of a diesel engine and the injection strategies of a common rail injector were simulated using CFD in that study. The 'original gas jet model' of Abani et al. (2008) and the 'normal gas jet profile model with breakup length formula' (NGJBL) of Lee et al. (2011) were each applied to KIVA-3V model and the computed outputs were compared. For model validation, CFD simulation results were compared with the multiple injection study results of Tennison et al. (1998) which is under a compression ratio of 18:1.

Lee & Reitz (2013) studied diesel spray tip penetration with CFD by reorganizing the compression ratio from the conventional compression ratio of a diesel engine, 18:1, to an ultra-high compression ratio of 100:1 as well as changing the gas densities. The spray tip penetration was CFD simulated by adopting both the 'Gas jet spray model', and 'Normal gas jet profile model with breakup length formula' (NGJBL model) into the KIVA-3V code. The spray tip penetration was CFD simulated for various spray patterns, such as single injection, pilot injection and split injection. The CFD simulation of the spray tip penetration with an 18:1 compression ratio was compared with a previous study with identical experimental conditions and showed that the 'Gas jet spray model' over predicted it. The CFD simulation results with the 'KIVA-3V Standard spray model' and the NGJBL model were generally in good agreement with the experimental data. The spray tip penetration was CFD simulated with the NGJBL model with step-by-step increased compression ratio. The spray tip penetration rapidly decreased for the range of compression ratio of 18:1–45:1 as the compression ratio increases and the spray tip penetration did not change much with increasing compression ratios in the range of 60:1–100:1. The CFD simulation results of the spray tip penetration, with respect to varying compression ratios, were generally in agreement with previous experimental studies.

García-Oliver et al. (2011) also contributed a study on the combined 1D-3D CFD approach on diesel spray calculations; nevertheless, little study on theoretical derivation of diesel spray with gas flow was reported. A 1D3D–CFD coupled spray model was proposed in that work for the simulation of Diesel sprays under non-evaporative conditions and constant injection velocity in time. The basic idea of the model was to reduce the poor estimations of the gas velocity and droplets/gas relative velocity obtained with the standard 3D–CFD Eulerian–Lagrangian spray model, when coarse meshes were used. The coupling has been achieved in the calculation of the momentum source interaction term. General considerations, descriptions and implementation of the model in a commercial CFD code were defined. Diesel spray simulations performed using the proposed approach have been compared with those obtained with the standard 3D–CFD, 1D models and experimental data. Encouraging results were found in terms of spray evolution when changing meshes and ambient conditions.

In the paper of Postrioti & Battistoni (2010), a detailed numerical and experimental analysis of a spray momentum flux measurement device capability was presented. Particular attention was devoted to transient, engine-like injection events in terms of spray momentum flux measurement. The measurement of spray momentum flux

in steady flow conditions, coupled with knowledge of the injection rate, was steadily used to estimate the flow average velocity at the nozzle exit and the extent of flow cavitation inside the nozzle in terms of a velocity reduction coefficient and a flow section reduction coefficient. In that study, the problem of analyzing spray evolution in short injection events by means of jet momentum flux measurement was approached. The research was based on 3D-CFD analysis with theoretical background of Momentum Conservations Equations of the spray target interaction in a momentum measurement device as below Figure 2.3.

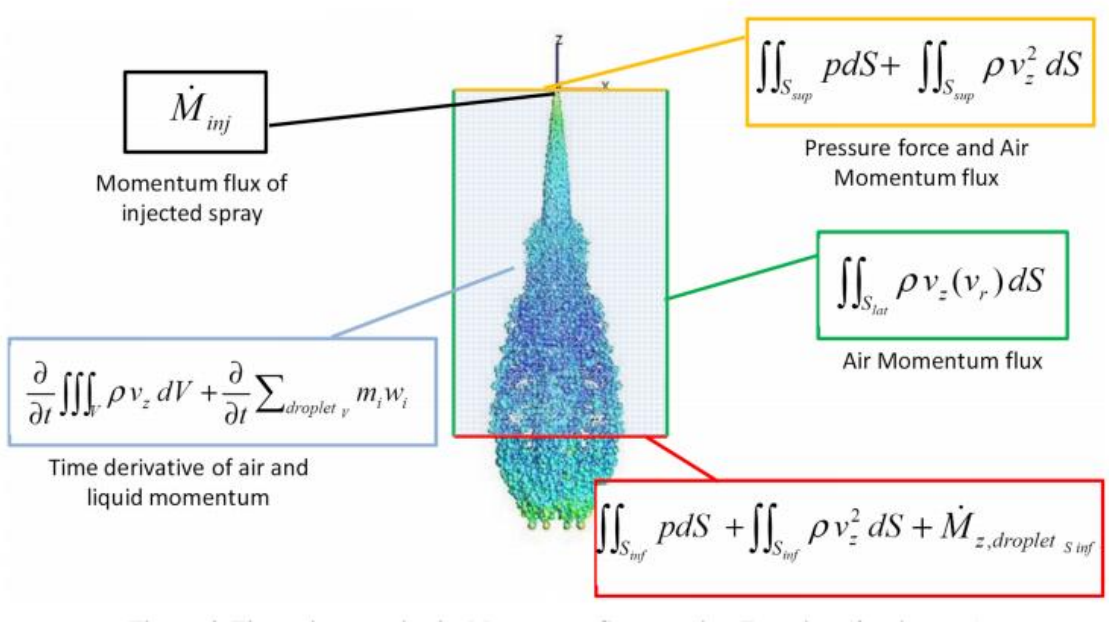

Figure 2.3. The main terms in the Momentum Conservation Equation (free jet case) (Source: Postrioti & Battistoni, 2010)

After a proper validation with experimental data (impact force time-history, spray penetration and cone angle obtained by spray imaging), the detailed analysis of the 3D flow field in different rig configurations and operating conditions led to significant awareness of the spray momentum measurement device operation. The obtained results showed that a properly designed momentum rig can be used for quantitative characterizations of the instantaneous momentum flux for each single jet in engine-like injection conditions, which are mostly important for the combustion process evolution in low-load conditions.

2.2. Artificial Neural Network (ANN)

Artificial Neural Networks are made up of simple elements of neurons operating in parallel which collect inputs and generate outputs. These elements are inspired by biological nervous systems. As in nature, the connections between elements mainly regulate the network function. A neural network is able to be trained to perform a specific function modifying the values of the connections (neurons in biology), namely weights, between elements.

Regularly, neural networks are regulated, or trained, so that a particular input guides to a specific target output. Here, the network is adjusted, based on a comparison of the output and the target, until the network output converges the target. Typically, many such input/target couples are required to train a network.

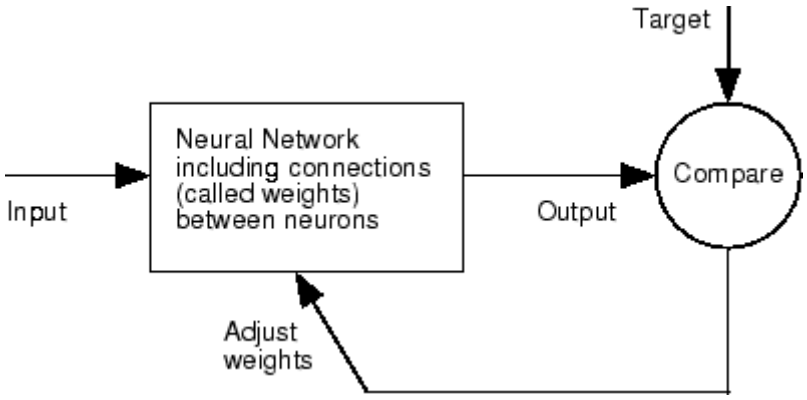

Figure 2.4. A typical neural network operating schema
(Source: Mathworks-ANN, 2016)

Neural networks have been trained to perform complex functions in various fields, including pattern recognition, identification, classification, speech, vision, control systems and simulations.

Neural networks can also be trained to solve problems that are tough for conventional computers or manual calculations. The ANN provides the use of neural network paradigms that build up to engineering, financial, and other practical applications (Mathworks, ANN, 2016).

Soft Computing is a common term for an aggregation of computing techniques (Zadeh, 1994). These well-known techniques comprise artificial neural networks, fuzzy

logic, evolutionary computation, machine learning and probabilistic reasoning in general. Soft computing methods separate from classical computing methods in terms of tolerance of imprecision, uncertainty, partial truth to achieve tractability, approximation, robustness, low solution cost and better rapport with reality (Das et al., 2013).

The genetic algorithm (GA) has been essentially applied in engine optimization field because of its potential in optimization which is based on natural selection, the process that drives biological evolution. The GA modifies a population of individual solutions again and again. At each step, the GA choses individuals at random from the current population to be parents and uses them to produce the children for the next generation. Over successive generations, the population "evolves" toward an optimal solution. The GA can be applied to solve a variety of optimization problems that are not well suited for standard optimization algorithms, including problems in which the objective function is discontinuous, non-differentiable, stochastic, or highly nonlinear. The GA can address problems of mixed integer programming, where some components are restricted to be integer-valued (Mathworks, GA, 2016). Furthermore, the GA is commonly used in order to reduce and optimize the reaction rate of combustion by reducing the number of involved species (Perini et al., 2012).

Levenberg-Marquardt (LM) is also a common algorithm used to solve especially non-linear least squares problems. The primary application of the LM algorithm is in the least squares curve fitting problem: given a set of *m* empirical datum pairs of independent and dependent variables, (x_i, y_i), optimize the parameters β of the model curve $f(x, \beta)$ so that the sum of the squares of the deviations becomes minimal as below equation:

$$S(\beta) = \sum_{i=1}^{m} [\, y_i - f(x_i, \beta)]^2 \qquad (2.1)$$

Taghavifar et al. (2014) investigated spray behaviour adopting along GA in ANN. Spray behaviour in the model was a function of nozzle and engine variant parameters such as crank angle, nozzle tip mass flow rate, turbulence and nozzle discharge pressure. The outputs tried to reach were spray penetration and sauter mean diameter (SMD) as below layer models.

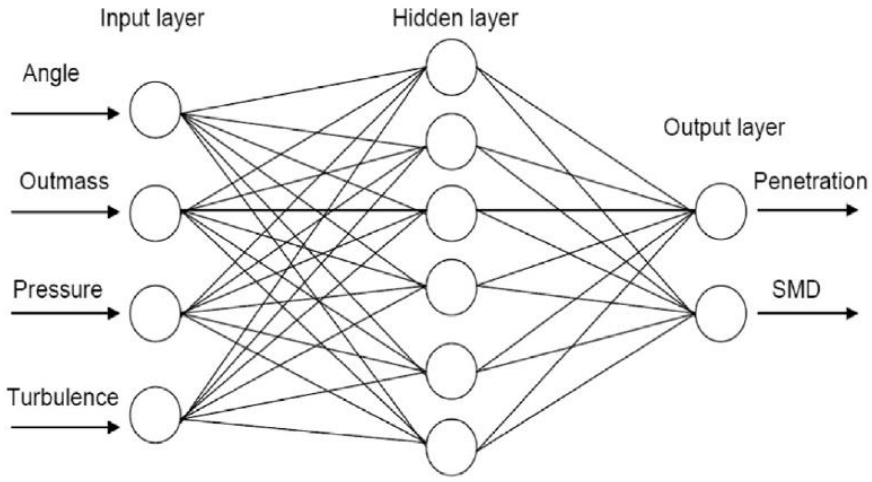

Figure 2.5. ANN structure with single hidden layer
(Source : Taghavifar et al., 2014)

The model was based on the experimental data which were used in specified conditions and the data acquired from CFD extrapolation. It was found that the LM algorithm had the least mean square error (MSE) for each ANN and the ANN-GA (ANN with genetic algorithm) models at 30 neurons in hidden layer with R^2 value of 0.998. Results also pointed out that the ANN-GA improved the spray specification modeling simply and with acceptable accuracy The ANN-GA and ANN performance comparison in terms of R^2 and MSE was as below:

Table 2.1. ANN-GA vs. ANN in the study of Taghavifar et al. (2014)

	ANN-GA	**ANN**
R2 (SMD-training)	0,998	0,992
MSE	0,3348	0,8994
Structure	4-30-2	4-24-2

Roy et al. (2014) presented the potential of ANN to predict the performance and exhaust emissions of an existing single cylinder four-stroke common rail direct injection (CRDI) engine under varying exhaust gas recovery (EGR) strategies using ANN based on experimental data. There were 4 input parameters which were load, fuel injection pressure, percentage of EGR and fuel injected per cycle.

The ANN model was developed to forecast 5 output parameters of brake specific fuel consumption (BSFC), brake thermal efficiency (BTE), CO_2, NO_X and particle matters (PM) in order to observe engine performance and emissions. The experimental data from CRDI setup and emission analyzer here were separated into three groups for the ANN model which were 70% for training the neural network, 15% for the network's cross-validation and remaining 15% for testing the performance of ANN. After implementing the data as input layer, the 2 hidden layers with 10 neurons for each were used to reach the output layer on the MATLAB platform. The ANN model was enabled to forecast the performance and emissions with excellent agreement with mean absolute percentage error in the range of 1.1 - 4.6%.

Cay et al. (2013) performed experimental investigations and then performed ANN validation over engine performance. They used the ANN to predict BSFC, AFR, emissions of CO and unburned hydrocarbons (UHC) of a spark ignition engine. The revealed experimental data of a four cylinder four stroke test engine operated at different engine speeds and torques were compared with the ANN modeling, the standard back propagation algorithm. The network structure was aimed for optimum choice of the training model. Four different algorithms of Quasi-Newton back propagation (BFGS), LM algorithm, resilient back propagation (RP) and scaled conjugate gradient learning algorithm (SCG) were used. The SCG learning algorithm gave optimal results with correlation coefficient (R^2) more than 0.99. After the studies, it was concluded that significant decrease in emission was observed with methanol however the engine performance was affected negatively due to methanol.

Liu et al. (2013) suggested an ANN approach for a new-fangled misfire detection model of a turbocharged diesel engine. An explicit back propagation neural network has been improved to identify diesel combustion misfire according to some engine operating parameters such as engine speed, intake temperature, boost pressure, exhaust temperature, water temperature and fuel consumption. The parameters were selected by using engine fault mode tree analysis. The proposed neural network model was implemented in MATLAB/Neural Network Toolbox. The mean square error of the training target was lower than 0,001.

Garg et al. (2012) worked on engine development research using an Artificial Neural Networks approach. They claimed that the ANN model resembles the logic in two premises:

- Knowledge is acquired by the network through a learning process
- Inter-neuron connection strengths known as synaptic weights are used to store the knowledge

They defined neural networks as parametrized computational non-linear algorithms for data/signal/image processing. The neural network was characterized by:

- Architecture
- Training or learning (determining weights on the connections)
- Activation function

Shamekhi et al. (2009) studied multi objective genetic algorithms to model several engine operations using Neural Networks. Multi objective optimization targets to find design variables like "x" that minimize or maximize "k" objective functions within "m" constraints. It could be formulated as follows (Ringuest, 1992; Samadani et al., 2008):

$$\min \vec{f}(\vec{x}) = (f_1(\vec{x}), f_2(\vec{x}), \dots, f_k(\vec{x}))^T \quad (2.2)$$
$$\text{s.t. } \vec{x} \in X = [\vec{x} \in R^n | u_j(\vec{x}) \leq 0 (j = 1, \dots, m)]$$

If the objective functions are in the trade-off relationship, it is strenuous to minimize or maximize all objective functions at the same time. In that case, the concept of superiority and Pareto optimum solution was suggested to be utilized (Shamekhi et al., 2009).

In the study of Najafi et al. (2016), some available studies using ANN and ANFIS have been compared with Najafi's study itself as in Table 2.2.

The correlation coefficient of ANFIS models (in grey) have been observed as producing more accurate results than ANN studies in the literature based on a correlation factor. This determination is one of the reason behind the election of ANFIS model instead of ANN model for this investigation which is also more practical explained in detail in the following pages.

Table 2.2. The comparison between several ANN and ANFIS studies

Ref.	Engine	Fuel type	Method	Input	Output	Best Performance
Sayın et al. (2007)	Gasoline	Gasoline with various octane number (91, 93, 95, 95.3)	ANN	Lower heating value, torque, speed, air inlet temperature	BSFC, BTE, exhaust gas temperature, CO, HC	R=0.996
Sharon et al. (2012)	Diesel	Biodiesel blend (B25, B50, B75, B100)	ANN	Power, bio-fuel blend	BSFC, BTE, Smoke number, CO, NOx, HC	R=0.999
Yusaf et al. (2010)	CNG-Diesel	Dual CNG–diesel fuel	ANN	Speed, fuel type	Power, torque, BSFC, BTE, NO_X, CO, CO2, O2, exhaust temperature	R=0.99
Cay, (2013)	Gasoline	Gasoline	ANN	Speed, torque, fuel flow rate, intake manifold mean temperature, cooling water inlet temperature	BSFC, power, exhaust temperature	R^2=0.99
Cay et al. (2013)	Gasoline	Gasoline, methanol	ANN	Speed, torque, fuel type, fuel flow	BSFC, CO, HC, air–fuel ration	R=0.999
Hosoz et al. (2013)	Diesel	Diesel–biodiesel blend (B0, B10, B20, B50, B75, B100)	ANFIS	Speed, load, fuel type	Power, BSFC, BTE, HC, CO, NO, exhaust gas temperature	R=1
Kiani et al. (2010)	Gasoline	Gasoline–ethanol blend (E0, E5, E10, E15, E20)	ANN	Speed, load, gasoline–ethanol blend	Power, torque, CO, CO2, NOx, HC	R=0.99
Canakci et al. (2009)	Diesel	Diesel–biodiesel blend (B5, B20, B50, B100)	ANN	Speed, fuel properties, environmental conditions	Flow rates, maximum injection pressure, emissions, engine load, maximum cylinder gas pressure, BTE	R^2=0.99

(Cont. on next page)

Table 2.2. (Cont.)

Ref.	Engine	Fuel type	Method	Input	Output	Best Performance
Roy & Ghosh et al. (2015)	Diesel	Diesel	Gene Expression Program	Load, fuel injection pressure, EGR, fuel injected per cycle	BSFC, BTE, CO2, NOx, PM	R=0.999
Ganesan et al. (2015)	Diesel Generator	Diesel	ANN	Speed, torque, load	CO2, CO/CO2, gross efficiency, flue gas temperature	R^2=0.999
Roy & Das et al. (2015)	Diesel	Diesel	ANFIS	Load, fuel injection pressure, CNG energy share	BSFC, BTE, NOx, PM, HC	R=0.999
Najafi et al. (2016)	Gasoline	Gasoline–ethanol blend (E0, E5, E10, E15, E20)	ANFIS	Speed, gasoline–ethanol blend	Power, torque, BTE, volumetric efficiency, BSFC, CO, HC, CO2, NOx	R=1

2.3. Adaptive Neuro-Fuzzy Inference System (ANFIS)

Theoretical background and modelling methodology of ANFIS are given in details in Chapter 3. It is a sort of artificial neural network which is based on Takagi–Sugeno fuzzy inference system (1985). Since it integrates both neural networks and fuzzy logic principles, it has the potential to catch the advantages of both in a single framework. Its inference system corresponds to a set of fuzzy IF–THEN rules that have the learning ability to simulate nonlinear functions. Thus and so ANFIS is regarded as a general figurer.

Najafi et al. (2016) studied a SI engine operating with ethanol gasoline blends of 0%, 5%, 10%, 15% and 20% namely E0, E5, E10, E15 and E20 respectively in order to disclose the use of support vector machine (SVM) and ANFIS to predict the performance parameters and the exhaust emissions. The engine was run at various speeds for each test fuel, and 45 different test conditions were created during the experiments. The brake

power, the engine torque, the brake thermal efficiency, and the volumetric efficiency are increased using ethanol blends, while the brake specific fuel consumption (bsfc) is decreased, when they were compared with neat gasoline fuel. Additionally, the concentration of CO and HC in the exhaust pipe decreased after ethanol blends were introduced, but CO_2 and NO_X emissions increased. In order to forecast the engine parameters, all the experimental data were arbitrarily divided into training and testing data. For the SVM modelling, different values for the radial basis function (RBF) kernel width and the penalty parameters (C) were considered, and the optimum values were then found. For the ANFIS modelling, 200 training epochs and the Gaussian curve membership function (gaussmf) were found to be the optimum choices for the training process. The results showed that the SVM predicted the engine performance and the exhaust emissions with the correlation coefficient (R) and the accuracy in the ranges of 0.66–1 and 65%–99%, respectively, while these same parameters were in the ranges of 0.76–1 and 79%-99%, respectively, for the ANFIS. The results demonstrate that the SVM and ANFIS are both capable of predicting the SI engine performance and emissions. Nevertheless, the performance of the ANFIS was obviously higher than that of the SVM.

The ANFIS, which is based on the Sugeno fuzzy inference model (SFIM), builds an input output mapping according to both the fuzzy "if" and "then" rules and the specified "input" and "output" data couples (Reddy & Mohanta, 2007). The "if" and "then" rules of the fuzzy system are usually employed to obtain the inference of an indefinite model, which could treat information in a system as well as experimental data. Using specific "input" and "output" training data couples, with the aid of sound membership functions, the "if" and "then" rules are structured. The ANFIS could arrange the membership function using the back-propagation gradient descent. The ANFIS simulated the Takagi–Sugeno–Kang (TSK) fuzzy rule of Type 3, where the consequent part of the rule is a linear combination of the inputs and a constant (Sugeno & Kang, 1988). The final output of the system is weighted by the average of each rules output. The form of the Type 3 rule used in the paper simulated in the system was as follows:

$$\text{If } x_1 \text{ is } A_1 \text{ and } x_2 \text{ is } A_2 \text{ and } \ldots x_p \text{ is } A_p,$$
$$\text{Then } y = c_0 + c_1 x_1 + c_2 x_2 + \cdots + c_p x_p$$

where [x1, x2, . . ., xp] are the input variables, [A1, A2, . . ., Ap] are fuzzy sets, which were settled during the training process, [c0, c1, . . ., cp] are the resultant parameters, and y is the output variable (Sisman-Yılmaz et al., 2004).

In the study of Najafi et al. (2016), the analysis was structured by also other methods such as multi layer perceptron (ANN-MLP), radial basis function (ANN-RBF) and support vector machine (SVM). After all the methods were applied, the accuracy and the errors were found in terms of correlation coefficient (R), root mean squar error (RMSE), Mean Relative Estimation Error (MRE) and accuracy in order to find the performance of those methods. The comparison of performance criteria among those methods has been tabulated as below:

Table 2.3. Performance comparison between the proposed and traditional methods (Source: Najafi et al., 2016)

Performance criteria	Method			
	ANN-MLP	ANN-RBF	SVM	ANFIS
R	0.708	0.735	0.835	0.918
RMSE	42.138	39.697	37.941	29.557
MRE	10.507	9.723	9.339	5.668
Accuracy	89.493	90.277	90.661	94.332

According to Table 2.3 above, it can be observed that ANFIS had better performances than the MLP based ANN and RBF based ANN and SVM in the prediction of the engine performance and exhaust emissions.

Baneshi et al. (2015) searched for the comparison of different network types in ANN. They selected best logs (for the sake of minimum information and maximum accuracy) for some parameters of hydrocarbon resources in oil and gas industry such as porosity, saturation, sonic, and density logs which are predicted by adaptive neuro fuzzy intelligence system, radial basis function, and artificial neural network models. The best models for each parameter were optimized and optimal epoch, neuron, function, and spread clarified. The parameters and indexes used in the models were density (RT), bulk density (RHOB), matrix density (DT) neutron log liquid filled porosity (NPHI), and formation water (SW).

The best correlation coefficient between target data and models output found when SE was input and RT and NPHI were outputs. Relative error percentage (REP) was minimum as 1.54% using DT & NPHI as inputs and RHOB as output in ANFIS model among ANN, RBF and ANFIS. Epoch 70 gave better results in terms of REP percentage during the study of finding the optimal epoch of network with try and error method in the epoch range of 0 – 200. One hidden layer with 12 neurons had the minimum error among the cases in the range of 0 - 22 neurons. For training functions, "trainlm" gave the lowest REP of test data of 6.76% among the bunch of membership functions (trainbfg, traincgp, traincgb, traincgf, trainoss, trainscg, trainrp, traingdx, traingda, traingd, traingdm). The optimum application points during neural network analysis are also tabulated as below as per their studies:

Table 2.4. The best method among Neural Network applications in the study of Baneshi et al. (2015)

Input Variables	Output Variabless	Model	Epoch	Neuron Numbers in Hidden Layer	Training Function	REP %
DT & NPHI	RHOB	ANFIS	70	12	trainlm	1.54%

Yetilmezsoy et al. (2011) studied the prediction of water-in-oil emulsions stability by ANFIS with basic compositional factors such as density, viscosity and percentages of SARA (saturates, aromatics, resins, and asphaltenes) components. In that study, it was noted that most of the regression models could not capture the non-linear relationships involved in the formation of these emulsions.

In the computational method, the optimum fuzzy rule base sets were generated by grid partition and subtractive clustering fuzzy inference systems. The stability estimation was carried on applying hybrid learning algorithm and the performance of the model was tested by the means of distinct test data set randomly selected from the experimental domain. The ANFIS-based forecasts in that study were compared to the common regression approach by means of various descriptive statistical indicators, such as root mean-square error (RMSE), index of agreement (IA), the factor of two (FA2), fractional variance (FV), proportion of systematic error (PSE), etc.

With trying various types of fuzzy inference system (FIS) structures and several numbers of training epochs ranging from 1 to 100, the lowest root mean square error

(RMSE = 2.0907) and the highest determination coefficient (R^2 = 0.967) were obtained with subtractive clustering method of a first-order Sugeno type FIS. For the optimum ANFIS structure, input variables were fuzzified with four Gaussian membership functions, and the number of training epochs was computed as 21. In the computational analysis, the predictive performance of the ANFIS model was examined for the following ranges of the clustering parameters: range of influence (ROI) = 0.45–0.60, squash factor (SF) = 1.20–1.35, accept ratio (AR) = 0.40–0.55, and reject ratio (RR) = 0.10–0.20. Results indicated that ROI, SF, AR and RR were obtained to be 0.54, 1.25, 0.50 and 0.15, respectively, for the best FIS structure. It was clearly concluded that the proposed ANFIS model demonstrated a superior predictive performance on forecasting of water-in-oil emulsions stability. Findings of that study clearly indicated that the neuro-fuzzy modeling could be successfully used for predicting the stability of a specific water-in-oil mixture to provide a good discrimination between several visual stability conditions.

Lee et al. (2007) investigated on that Adaptive Neuro-Fuzzy Inference System (ANFIS) fundamentally compensates the requirement for manual optimisation of the fuzzy system parameters. System parameters were automatically adapted by a neural network; for example, the membership function boards, leading to improved performance without operator intervention. In the ANFIS model, the estimation of spray penetration length and cone angle could be developed because the conjunction of neural network and fuzzy logic enabled the system to train itself and to improve its results based on experimentally available data. The neuro fuzzy system with the training capability of a neural network and with the advantages of the rule oriented fuzzy system could improve the performance significantly and provide a model in order to integrate the experienced observations into the categorization process.

Ultimately, Table 2.5 below also summarizes the current researches using ANFIS model for combustion characteristics validating experimental and/or CFD studies. The table includes engine types which are generally compression ignition, input parameters, output parameters, membership function types and the performance values in terms of R^2, RMSE, MRE and accuracy. According to these results, MF type of gaussmf, gbellmf and trapmf have more accurate results than gauss2mf and psigmf for this kind of analyses. The performance values are conditionally formatted and colored in the table at right most coloumns. In the light of these studies, the results are separately evaluated to determine the parameters of this main study.

Table 2.5. Various ANFIS models simulating combustion with their performance

Ref.	Eng. Type	Inputs	Outputs	Input MF	Performance Criteria			
					R^2	RMSE	MRE (%)	ACC. (%)
Najafi, (2016)	CI	Speed (rpm), Ethanol blend ratio (%)	Power (kW), Torque (N.m), BSFC (g), Volumetric Efficiency (%), BTE (%), CO, HC, CO2, NOx	gaussmf	1.00	0.51	1.19	98.8
Najafi, (2016)	CI	Speed (rpm), Ethanol blend ratio (%)	Power (kW)	gbellmf	1.00	0.76	1.71	98.3
Najafi, (2016)	CI	Speed (rpm), Ethanol blend ratio (%)	Power (kW)	trapmf	1.00	0.96	2.36	97.6
Roy, (2015)	CI	Load (%) Fuel Injection Pressure (Mpa) CNG Energy Share (%)	BSFC (g/kW.h), BTE (%), NOx (g/kW.h), PM (g/kW.h), HC (g/kW.h)	gaussmf	1.00	0.91		
Roy, (2015)	CI	Load (%) Injection timing (°) LPG content (%)	BSEC (kJ/kWh)	trapmf gbellmf trimf	0.99	0.10		93.3
Roy, (2015)	CI	Load (%) Injection timing (°) LPG content (%)	BTE (%)	gauss2mf gbellmf psigmf	0.98	0.11		86.7
Roy, (2015)	CI	Load (%) Injection timing (°) LPG content (%)	EGT (°C)	gauss2mf trimf	0.98	0.31		93.3
Roy, (2015)	CI	Load (%) Injection timing (°) LPG content (%)	Smoke (Hartridge Smoke Unit)	trimf gbellmf	0.93	0.23		46.7
Baneshi, (2015)	-	DT (Density Log) NPHI (Liquid Filled Porosity) RHOB (Bulk Density)	PHIE				7.48	
Baneshi, (2015)	-	DT NPHI	RHOB--				1.54	
Baneshi, (2015)	-	NPHI RHOB	DT				2.82	
Baneshi, (2015)	-	RT NPHI RHOB DT	SW (Formation Water)				30.38	
Baneshi, (2015)	-	RT NPHI RHOB DT	SW (Formation Water)				30.38	

(Cont. on next page)

Table 2.5. (Cont.)

Ref.	Eng. Type	Inputs	Outputs	Input MF	Performance Criteria			
					R^2	RMSE	MRE (%)	ACC. (%)
Mariani, (2014)	CI	EGR Valve Position (%) Lambda probe (-) VGT Control Valve Position (%)	Volumetric Oxygen Concentration (%)	trimf		0.18	4.50	
Mariani, (2014)	CI	EGR Valve Position (%) Lambda probe (-) VGT Control Valve Position (%)	Volumetric Oxygen Concentration (%)	gaussmf		0.24	13.50	
Mariani, (2014)	CI	EGR Valve Position (%) Lambda probe (-) VGT Control Valve Position (%)	Volumetric Oxygen Concentration (%)	trimf		0.26	7.00	
Hosoz, (2013)	CI	Speed (rpm) Load (%) Biodiesel content (0% to 100%)	Brake power (kW), Exhaust gas temperature (°C), BSFC (g/kWh), BTE (%), HC, CO, NO,		1.00	0.09	1.40	
Yetilmezsoy, (2011)	CI	Density Viscosity Additives of SARA	Emulsion stability	gaussmf	0.97	2.09		
Lee, (2007)	CI	Pressure (Mpa) Density (kg/m3)	Penetration (mm)	trimf	1.00			

In this study, an adaptive neuro-fuzzy model is developed for the study of the effects of water-in-diesel emulsions on diesel sprays. The model is validated by two separate papers based on experimental study and one paper based on CFD analysis focusing on combustion performance and spray behaviours. The effects of chamber pressure, injection pressure, and ambient temperature are also investigated as well as emulsion, namely diesel-water fraction.

CHAPTER 3

MATERIAL & METHODOLOGY

3.1. Material: Emulsion

A diesel fuel emulsion is a well-mixed type of diesel fuel with water. Diesel, namely automotive gasoil (AGO), is defined as “continues phase” in the mixture whereas the water is defined as “dispersed phase”. In various applications, it is observed that water is added to the diesel fuel in the range of 10–30% by mass or volume (Barnaud et al., 2000). A small amount of emulsifier usually in the range 1–5% is used to stabilize the emulsion increasing its kinetic stability. A class of emulsifier is also called as surfactant; this name comes from surface active agents.

An emulsifier, or surfactant, is a matter which is adsorbed at the interface of the system and alters the inter-facial free energy of the interface. In general, a hydrophilic surfactant with a certain hydrophilic-lipophilic-balance (HLB) value is added into water for decreasing the interfacial tension and retarding the aggregation, concentration, and creaming between oil and water phases. Meanwhile, a lipophilic surfactant is added into diesel to stabilize the oil phase. A magnetic stirrer is mostly used to mix and heat the water and diesel while hydrophilic and lipophilic surfactants were added in separately (Huo et al., 2014; Emberson et al., 2016). After using surfactant, the emulsion of diesel fuel with water can be utilized in the CI engine as regular fuel.

In various studies, it is shown that the use of diesel fuel emulsions reduces NO_X, CO, soot, hydrocarbons (HC) and PM emissions (Fahd et al., 2013; Lin & Chen, 2008; Maiboom & Tauzia, 2011; Nadeem et al., 2006; Liu et al., 2011; Armas et al., 2005; Park & K. Y. Huh, 2000; Qi et al., 2010). Fuel emulsification is regarded as a potential solution to the emission issues and it has received much attention in the last decades (Valdmanis & Wurlfhorst, 1970; Song & Lee, 2000; Musculus et al., 2003; Kadota & Yamasaki, 2002; Lin & Lin, 2007). Additionally, it has been showed that the brake thermal efficiency of a CI engine is slightly improved using emulsion as fuel (Armas et al., 2005; Qi et al., 2010; Abu-Zaid, 2004; Lif & Holmberg, 2006).

There has been very little work done researching the spray behaviours of diesel fuel emulsions, which causes the general lack of understanding concerning their use in direct injection CI engines. This study goes some way to address this through the ANFIS modelling of various experimental studies on diesel fuel emulsion sprays. For this aim, a few spray parameters, i.e. chamber pressure, injection pressure, ambient temperature and diesel-water fraction, are used to find out the effects on the spray cone angle and the spray tip penetration.

3.2. Methodology

3.2.1. Theoretical Background of Anfis

In a neural network model, the training set data basically builds the system. However, using a neuro-fuzzy configuration, the system is built by fuzzy logic definitions and then it is refined using neural network training algorithms. For the architecture of the model, ANFIS have membership functions and rules to be designed fed by the experimental data employing human knowledge, experience about the target system to be exploited. The ANFIS can then refine the fuzzy with 'if-then' rules and membership functions to describe the input-output behaviour of a complex system. In practical applications Sugeno type FIS models have been considered which are more suitable for constructing fuzzy models due to their more compact and computationally efficient representation of data than the Mamdani fuzzy systems (Lee et al., 2007). A typical zero-order Sugeno fuzzy system has the form as below:

$$\text{If } x \text{ is } A \text{ and } y \text{ is } B, \text{ then } z = c. \tag{3.1}$$

where A and B are fuzzy sets and z is a sharply defined function. Alternatively, a more general first-order Sugeno can be used by setting to a higher order function:

$$z = px + qy + c. \tag{3.2}$$

However, a higher order system of times brings an unjustifiable level of complexity because of the algorithm needed to optimise the parameters. For this reason,

a zero-order Sugeno FIS is used in most of the investigations. Figure 3.1 demonstrates the equivalent ANFIS architecture which consisted of five layers (Jang, 1993):

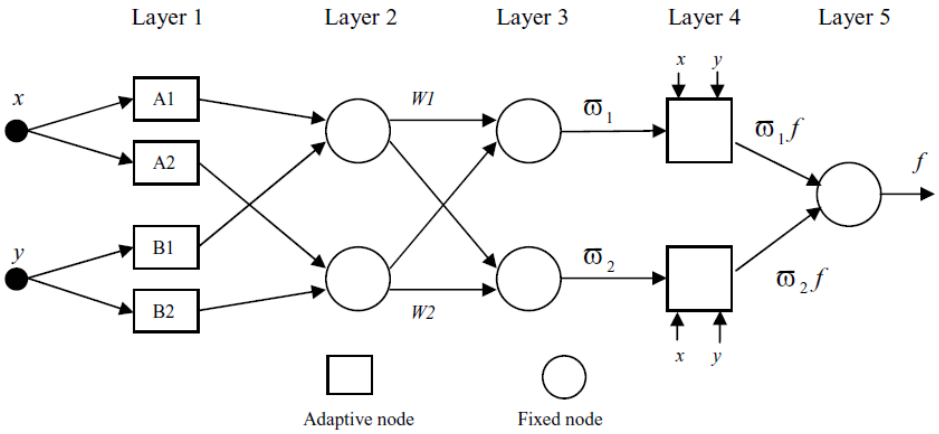

Figure 3.1. ANFIS Sugone Fuzzy System
(Source: Jang, 1993)

Variables *x* and *y* correspond to input values of *A1*, *A2* and *B1*, *B2* respectively in the Layer 1. *A1*, *A2*, *B1* and *B2* can be either the linguistic labels (small, large, high, low etc.) as well as numerical values used in the fuzzy theory for dividing the membership functions. The membership relationship between the output and input in this layer can be expressed as:

$$O_{1,i} = \mu_{Ai}(x),\ i = 1,2 \tag{3.3}$$

$$O_{1,j} = \mu_{Bj}(x),\ j = 1,2 \tag{3.4}$$

where $O_{1,i}$ and $O_{1,j}$ represent the output functions, μ_{Ai} and μ_{Bj} are the membership functions.

Layer 2, commonly referred to as the 'rule layer' consists of two fixed nodes in Figure 3.1 above which represent the fuzzy strengths of each rule. The product rules can be used to calculate the weighting function for the fuzzy operator 'AND' of a Sugeno FIS.

The output W1 and W2 are the weight functions for the next layer. The input and output relationship in this layer is:

$$O_{2,i} = W_i = \mu_{Ai}(x)\,\mu_{Bi}(y),\ i = 1,2 \tag{3.5}$$

where $O_{2,i}$ is the output of second layer.

The third layer is the normalised layer and its function is to normalise the weight function:

$$O_{3,i} = \varpi_i = \frac{\omega_i}{\omega_1+\omega_2},\ i = 1,2 \tag{3.6}$$

where $O_{3,i}$ is the output of third layer.

The fourth layer holding the adaptive nodes is the defuzzification layer. The output from this layer is "$\varpi(px + qy + r)$", where p_i, q_i and r_i are the consequent parameters of the node. The input and output relationship in this layer can be defined as:

$$O_{4,i} = \varpi_i f_i = \varpi_i(p_i x + q_i y + r_i),\ i = 1,2 \tag{3.7}$$

where $O_{4,i}$ is the output of the fourth layer.

The fifth layer consists of a single fixed node which is the summation of the weighted output of the consequent parameters in layer 4. The output layer is given by:

$$O_{5,i} = \sum_i \varpi_i f_i = \frac{\sum_i \omega_i f_i}{\sum_i \omega_i},\ i = 1,2 \tag{3.8}$$

The nodes in the input layer are adaptive. Any appropriate membership functions can be used for the system. In the study, "trimf", "pimf", "gaussmf" are chosen in general to describe the parameters due to their smoothness and direct notation (Lee et al., 2007).

The triangular MF (trimf) is formally expressed as (Mariani et al., 2014):

$$MF(x,a,b,c) = f(x,a,b,c) = \begin{cases} 0, & x \le a \\ \frac{x-a}{b-a}, & a \le x \le b \\ \frac{c-x}{c-b}, & b \le x \le c \\ 0, & c \le x \end{cases} \tag{3.9}$$

where x is one of the four input variables in the first layer and the parameters a, b and c describe the shape of the triangular MF.

The symmetric Gaussian MF (gaussmf) is expressed as (Mariani et al., 2014):

$$MF(x,\sigma,c) = f(x,\sigma,c) = e^{\frac{-(x-c)^2}{2\sigma^2}} \tag{3.10}$$

Where the function is dependent on the two parameters of σ and c, while x is one of the four input variables in the first layer.

The Π -shaped built-in MF (pimf) is a spline-based curve so named because of its Π shape (can be seen from Figure 3.2). The membership function is evaluated at the points determined by the vector x. The parameters a and d locate the "feet" of the curve, while b and c locate its "shoulders." It is expressed as below (Mathworks, FUZZY, 2016):

$$f(x;a,b,c,d) = \begin{cases} 0, & x \le a \\ 2\left(\frac{x-a}{b-a}\right)^2, & a \le x \le \frac{a+b}{2} \\ 1-2\left(\frac{x-b}{b-a}\right)^2, & \frac{a+b}{2} \le x \le b \\ 1, & b \le x \le c \\ 1-2\left(\frac{x-c}{d-c}\right)^2, & c \le x \le \frac{c+d}{2} \\ 2\left(\frac{x-d}{d-c}\right)^2, & \frac{c+d}{2} \le x \le d \\ 0, & x \ge d \end{cases} \tag{3.11}$$

Trapezoidal-shaped membership function (trapmf), based on a trapezoidal curve, is a function of a vector, x, and depends on four scalar parameters *a*, *b*, *c*, and *d*, as given by (Mathworks, FUZZY, 2016):

$$f(x;a,b,c,d) = \max\left(\min\left(\frac{x-a}{b-a}, 1, \frac{d-x}{d-c}\right), 0\right) \tag{3.12}$$

Difference between two sigmoidal functions membership function (dsigmf) is a sigmoidal membership function depends on the two parameters *a* and *c* expressed as below (Mathworks, FUZZY, 2016):

$$f(x; a, c) = \frac{1}{1+e^{-a(x-c)}} \tag{3.13}$$

The membership function dsigmf depends on four parameters, a1, c1, a2, and c2, and it is the difference between two of these sigmoidal functions:

$$f1(x;\ a1, c1)\ -\ f2(x;\ a2, c2) \tag{3.14}$$

Generalized bell-shaped membership function (gbellmf) is a generalized bell function depends on three parameters *a*, *b*, and *c* as given by (Mathworks, FUZZY, 2016):

$$f(x; a, b, c) = \frac{1}{1+\left|\frac{x-c}{a}\right|^{2b}} \tag{3.15}$$

where the parameter b is usually positive. The parameter c locates the center of the curve. Enter the parameter vector params, the second argument for gbellmf, as the vector whose entries are a, b, and c, respectively.

The plot below reveals the structure type of the all membership functions in use:

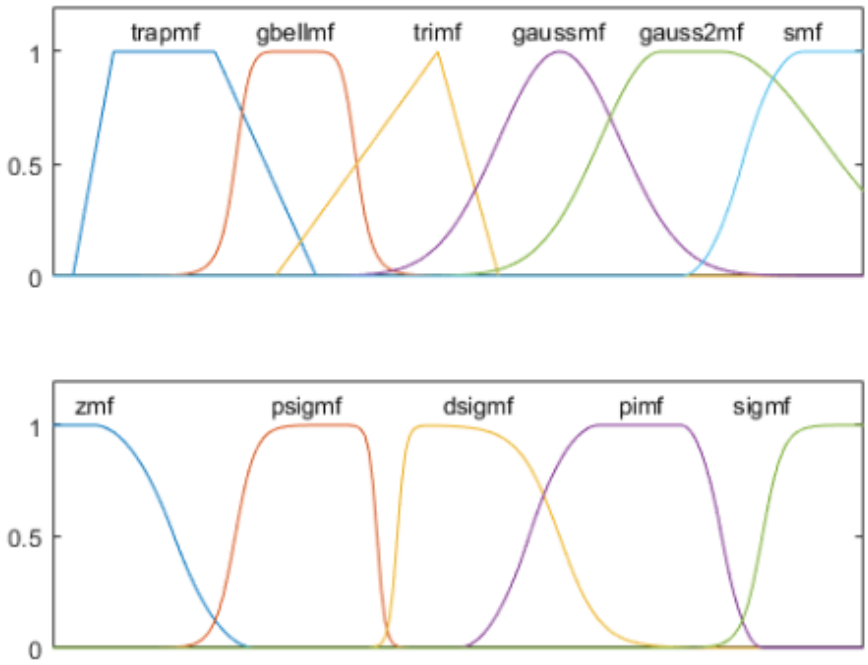

Figure 3.2. A plot view of the membership functions used in ANFIS

Another main term during applying ANFIS model into MATLAB is the “epoch” number. The training process stops if the designated epoch number is reached or the error goal is achieved, whichever comes first.

3.2.2. Anfis Modelling in Matlab

ANFIS is fundamentally a training programme for Sugeno-type fuzzy inference system. It uses a mixture learning algorithm to tune the parameters of neural network and a Sugeno-type fuzzy inference system (FIS). The algorithm employs a hybrid of the least-squares and back-propagation gradient extraction methods to model a training data set. ANFIS additionally corroborates models using a controlling data set to test for overfitting of the training data (Jang, 1993).

The ANFIS methodology is applied with the software of MATLAB R2011a during this study since its accuracy and consistency is verified by several studies in the literature (Mariani et al., 2014; Roy et al., 2015; Liu et al., 2013). The below commands and applications are the tools used in Matlab (Mathworks, ANFIS, 2016):

Input arguments for anfis are:

- trnData: Training data, defined as a matrix. For an FIS with N inputs, trnData has “N+1” columns, where the first N columns hold input data and the final column comprises output data.
- initFis: FIS structure utilized to state a primary set of membership functions for training, specified as one of the following:
    - Positive integer: Sets the number of membership functions for all inputs and creates an initial FIS using genfis1.
    - Vector of positive integers: Sets the number of membership functions for each input separately and creates an initial FIS using genfis1.
    - An FIS structure, produced using genfis1 or genfis2, that fulfils conditions below:
        - First or zeroth order Sugeno-type system.
        - Single output, acquired using weighted average defuzzification. All output membership functions must be the same type and be either linear or constant.

- No rule sharing. Dissimilar rules cannot use the same output membership function.
- Unity weight for each rule.
- No custom membership functions or defuzzification methods.

Unless "initFis" is defined, ANFIS utilizes genfis1 to produce a default initial FIS for training. The default FIS contains two Gaussian MF for each input.

- trnOpt: Training options, specified as a vector of scalars that represent the options below:
  - trnOpt(1) — Training epoch number (default: 10)
  - trnOpt(2) — Training error target (default: 0)
  - trnOpt(3) — Initial step size (default: 0.01)
  - trnOpt(4) — Step size decrease rate (default: 0.9)
  - trnOpt(5) — Step size increase rate (default: 1.1)

The training process stops when it reaches the designated epoch number or achieves the training error goal. Then, display options (dispOpt) are applied to specify information in the Command Window.

Output arguments for ANFIS are as followings:

- FIS: FIS structure whose parameters are adjusted using the training data, returned as a structure.
- Error: Root mean squared training data errors at each training epoch, returned as an array of scalars.
- Stepsize: Step sizes at each training epoch, returned as an array of scalars.
- chkFis — FIS structure that corresponds to the epoch at which chkErr is minimum.
- chkErr — Root mean squared checking data errors at each training epoch, returned as an array of scalars.

In this study, the ANFIS models are applied selecting the 80% of data for training dataset and 20% for test dataset, leaving maximum and minimum values in the training dataset. The datasets are extracted from the figures of the papers explained in "Chapter 4 – Data" in details. Afterwards the program is employed using tools above and results of 3D surfaces and scatter plots are displayed in order to reach the results.

3.2.3. Performance Criteria

In order to evaluate the performance of a method in prediction, several criteria are calculated. The criteria used in this study are the correlation coefficient (R), the root mean square error (RMSE), and the accuracy. R evaluates the strength of the relationship between the experimental and predicted results (Najafi et al., 2016), is defined as:

$$R(a,p) = \frac{cov(a,p)}{\sqrt{cov(a,a)cov(p,p)}} \tag{3.16}$$

where $cov(a,p)$ is the covariance between sets a and p. a and p denote the actual output and forecasted output sets, individually (Sayin et al., 2007).

RMSE is determined as follows:

$$RMSE = \sqrt{\frac{1}{n}\sum_{i=1}^{n}(a_i - p_i)^2} \tag{3.17}$$

where n is the number of the points in the data set.

Accuracy, a simple representation of prediction performance (Widodo & Yang, 2011), is calculated as follows:

$$Accuracy = \left(\frac{a_i - p_i}{a_i}\right).100 \tag{3.18}$$

where a_i is the actual value and p_i is the forecasting value, namely simulation results in our study.

CHAPTER 4

EXPERIMENTAL DATA RESOURCES

4.1. Selecting the Base Studies from Literature

In this thesis, the spray characteristics in terms of spray penetration and angle has been investigated using Sugeno approach in ANFIS model via Matlab R2011a based on two studies namely experimental data in the literature. The experimental investigations are also covering the emulsion analysis since they are looking for the spray and combustion characteristics of water-emulsified diesel which can be correlated with the aim of this thesis.

The dynamics and effects of the inputs gathered from both experimental and numerical studies are tried to be understood over the spray penetration at the same time.

The studies are:

- "*Optical characterization of Diesel and water emulsion fuel injection sprays using shawdography*" by D. R. Emberson, B. Ihracska, S. Imran and A. Diez in 2016 published by Fuel vol:172.
- "*Study on the spray and combustion characteristics of water–emulsified diesel*" by Ming Huo, Shenlun Lin, Haifeng Liu and Chia-fon F. Lee in 2014 published by Fuel vol:123

After refining the data from the sources above, they were utilized in the model using the process given in details in the following sections.

4.2. Experimental Data

To begin with the detailed description of data gathering, we provide the main properties of two data sources which note variables as “Var.” and constants as “Const.” with their units in box brackets in Table 4.1. below:

Table 4.1. Model Progress Data Sets

	Ambient Pressure	Fuel Diesel Fraction	Injection Pressure	Chamber Temperature	Time	Nozzle Diameter	Nozzle Hole Numbers	Nozzle Hole Length	Nozzle Hole Diameter	Nozzle Hole Angle	Spray Cone Angle	Spray Penetration
Emberson, (2016)	**[bar] Var**	**[%] Var**	**[bar] Var**	[°C] Const	**[µs] Var**	[µm] Const	[ ] Const	[µm] Const.	[µm] Const	[deg] Const	[deg] Output	**[mm] Output**
Huo, (2014)	[bar] Const	**[%] Var**	[MPa] Const	**[K] Var**	**[µs] Var**	N/A	[ ] Const	N/A	[µm] Const	N/A	N/A	**[mm] Output**

Among the data above consisting of 10 different inputs and 2 different outputs at all, this study focused on the variable ones while excluding the constant ones noted as “Const.” and not available ones noted as “N/A”. The reason behind this selection is the motivation to analyze the effects of the inputs over the output in which the inputs are required to be varying whilst outputs are changing.

In the first data set, which is obtained from Emberson study (Emberson et al., 2016), the spray penetration data are extracted in detail from Figure 4.1 and Figure 4.2 below generated using the shadowgraph image sequences in that study. The cases are separated in terms of their emulsion rates as D (100% Diesel), D10 (90% Diesel + 10% Water) and D20 (80% Diesel + 20% Water) and their chamber pressure and fuel injection pressure. Hereby, the neat diesel fuel has the properties of the density of 814 kg/m^3 and the viscosity of 0.00588 Pa.s.

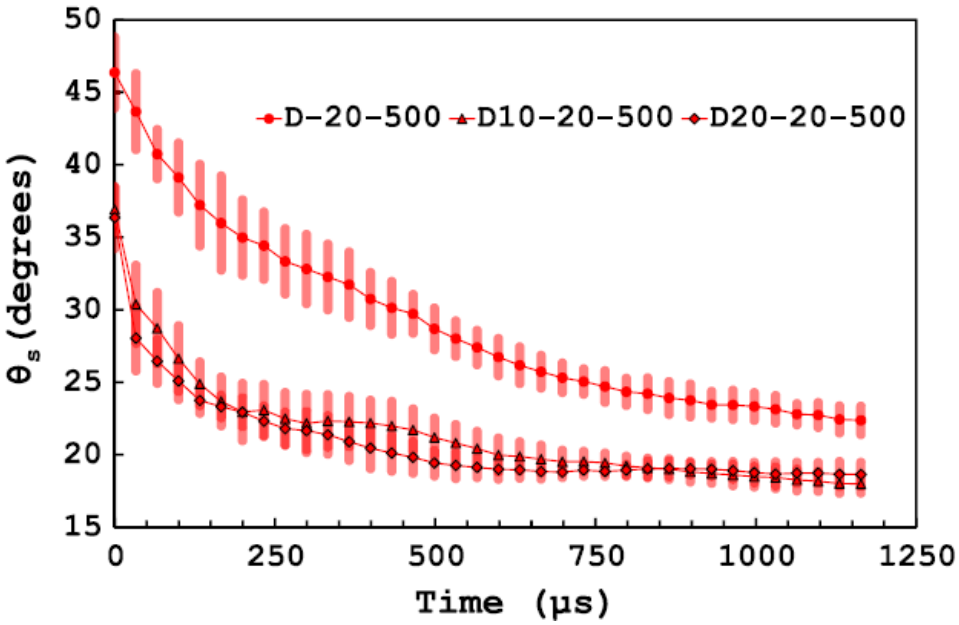

Figure 4.1. Fuel injection spray angle with time for varying fuel types at P_{amb}=20bar and P_{inj}=500bar (Source: Emberson et al., 2016)

Figure 4.1 have been attained during the experiments to find the injection spray angles with time for varying fuel types, namely emulsion rates, while the chamber ambient pressure is 20 bar which corresponds to the ambient gas density of 22.6 kg/m^3 and the injection pressure is 500 bar. This study has been repeated while the ambient pressure is 30 bar which subtends to the ambient gas density of 34.5 kg/m^3 and the injection pressures are 700 bar and 1000 bar. Error bars are the magnitude of one standard deviation for the 15 injections used for determining the average.

Figure 4.2 of Emberson et al. (2016) depicts the spray penetration values for the same scenarios used in fuel injection spray angles, again determined using the shadowgraph image sequences.

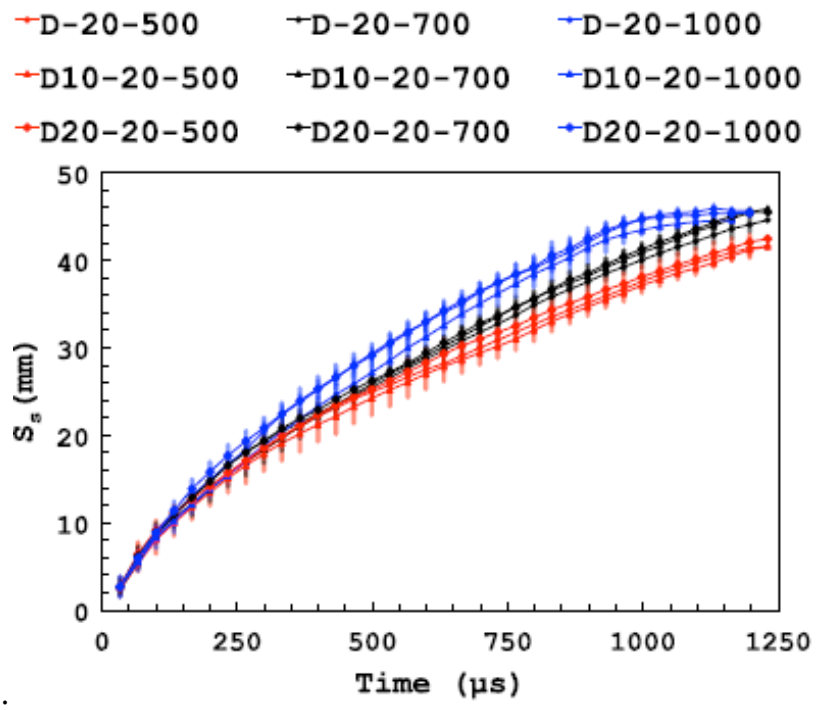

Figure 4.2. Fuel injection spray tip penetration variation with time after SOI for Diesel fuel, D10 and D20 when P_{amb} is 20 bar and P_{inj} are 500, 700 and 1000 bar respectively (Source: Emberson et al., 2016)

Spray penetration values are available as well for P_{amb} of 30 bar in with the same density values given mentioned above. Error bars corresponding to one standard deviation.

The independent variable inputs are taken into account to see the varying effects of the inputs over the output of spray penetration. In the data set obtained by Emberson et al. (2016), the nozzle geometrical details and chamber ambient temperature were constant inputs. Among the variable inputs, ambient gas density, fuel fraction, density, viscosity, injected fuel mass and injection duration were dependent on rest of the variables; therefore, they are also excluded in this study. The independent variable inputs are taken into account among inputs because the marginal effects on outputs can be observed only with these parameters. Therefore, the chamber ambient pressure, fuel diesel fraction, injection pressure and time after start of injection are taken into account during the simulations shown as “independent variable inputs” to reach the outputs of spray penetration and spray angle as in Figure 4.3 below:

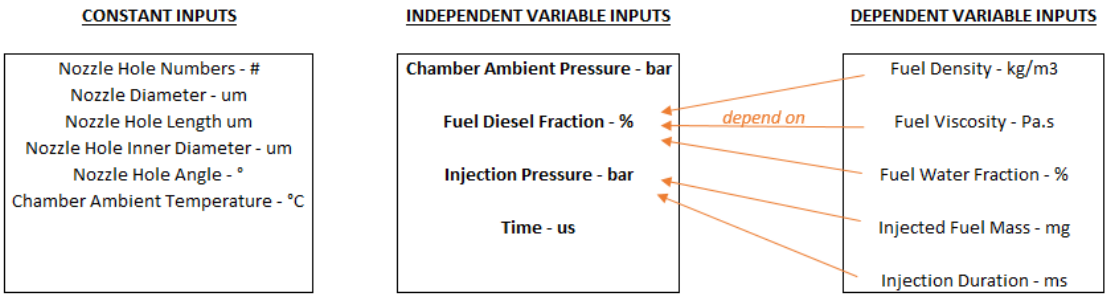

Figure 4.3. Constant and variable inputs of the data in Emberson et al. (2016)

Data from Figure 4.2 and other variations are then tabulated separately to be used in the ANFIS analysis as explained in Chapter 3. From the study of Emberson et al. (2016) all the 2155 data are extracted to be used in the ANFIS models. They are also tabulated below displaying only the extreme values.

Table 4.2. The dataset from Emberson et al. (2016)

Chamber Ambient Pressure bar	Fuel Diesel Fraction -	Injection Pressure bar	Time us	Penetration mm
20	1.0	500	0	0.0
20	0.9	500	0	0.0
20	0.8	500	0	0.0
30	1.0	500	0	0.0
30	0.9	500	0	0.0
.	.	.	.	.
.	.	.	.	.
.	.	.	.	.
20	1.0	1000	1050	45.2
20	0.8	1000	1050	45.2
20	0.8	1000	1100	45.4
20	1.0	1000	1150	46.0
20	0.8	1000	1150	46.0

The second data set for this study is shown in Figure 4.4 from Huo et al. (2014). They presented a study of the effect of water content in emulsions as well as the effect of ambient temperature on sprays focussing on the effects of ambient temperatures which are 800 K and 1200 K, and various emulsion rates, in which the indicating number

represents the volumetric ratio of water that are neat ULSD (ultralow sulphur diesel), W10 (90% ULSD + 10% Water) and W20 (80% ULSD + 20% Water) over the spray penetration amount. The neat ULSD fuel has the properties of the density of 840 kg/m^3 and the viscosity of 0.00252 Pa.s. The images showing inside the combustion chamber are from the start of the injection with a time interval of 67 μs between consecutive images. The quantitative measurement of the liquid penetration, based on the leading edge detection from the images, is shown in Figure 4.4 below:

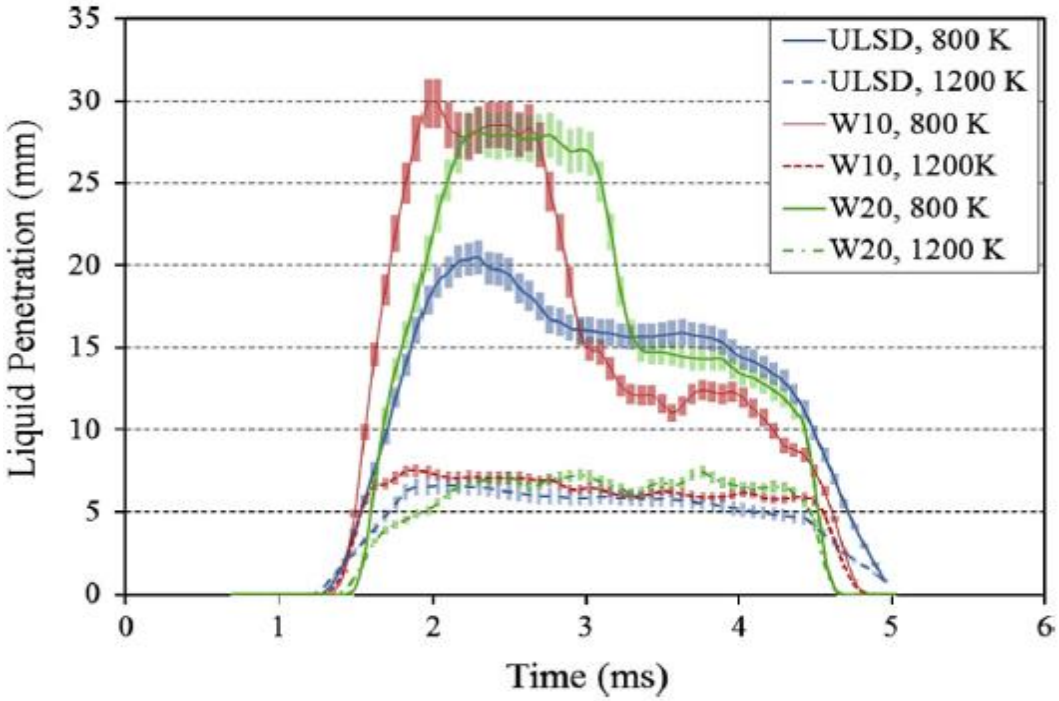

Figure 4.4. Liquid penetration under various ambient temperatures of 800K and 1200K and various fuel types in Huo et al. (2014)

From this study, the independent variable inputs selected are chamber ambient temperature, time and diesel fractions, in the simulations to reach the output of penetration as shown in Figure 4.5.

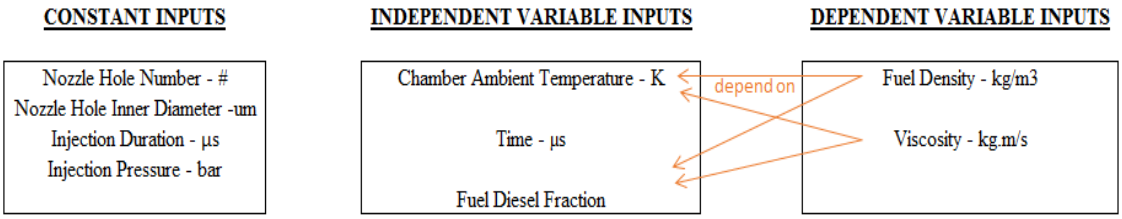

Figure 4.5. Constant and variable inputs of the data in Huo et al. (2014)

The data for spray penetration in Figure 4.4 are then tabulated separately for the ANFIS analysis as explained in Chapter 3 using the independent variable inputs mentioned above. Totally 244 data extracted from Huo et al. (2014) which is used in the ANFIS model. The dataset is displayed below Table 4.3 only with end values.

Table 4.3. The dataset from Huo et al. (2014)

Chamber Ambient Temperature °C	Fuel Diesel Fraction -	Time µs	Penetration mm
527	1	0	0.0
527	1	80	1.3
527	1	160	3.0
527	1	240	5.5
527	1	320	7.8
.	.	.	.
.	.	.	.
.	.	.	.
927	0.8	560	5.0
927	0.8	640	5.5
927	0.8	720	6.3
927	0.8	800	6.8
927	0.8	880	6.9

As final modelling, the dataset of Emberson's and Huo's studies are combined shown in Table 4.4; to find the effects of ambient temperature over spray penetration which is currently not available in Emberson's study. In Emberson's study, only the 298 K of ambient temperature is investigated during its experiments. Thanks to the simulation,

ambient temperature values of 800 K and 1200 K are also modelled benefitting from the results of Huo's study. Thereby the study of Emberson is repeated with new ambient temperature conditions through the simulation.

There are number of 394 rows and 2.364 data extracted from studies to be used in the ANFIS model. The dataset is displayed only with extreme values as below:

Table 4.4. The combined dataset of previous experimental studies

Chamber Ambient Pressure bar	**Fuel Diesel Fraction -**	**Injection Pressure bar**	**Time µs**	**Chamber Ambient Temperature °C**	**Penetration mm**
20	1	500	0	25	0.0
20	1	700	0	25	0.0
20	0.9	700	0	25	0.0
20	0.8	700	0	25	0.0
20	0.8	500	0	25	0.0
.	.	.	.	.	.
.	.	.	.	.	.
.	.	.	.	.	.
51	1	700	240	927	2.2
51	1	700	320	927	3.0
51	1	700	400	927	4.0
51	1	700	480	927	5.0
51	1	700	720	927	6.5

All the figures and data mentioned above in two studies are then tabulated to utilize following the ANFIS Sugeno approach in MATLAB R2011a to forecast in an adaptive neuro-fuzzy modeling for the effects of water-in-diesel emulsions on diesel sprays.

CHAPTER 5

RESULTS AND DISCUSSION

This study mainly focuses on two objectives, the first is finding the most accurate model in terms of root mean square error (RMSE) after setting the ANFIS properties (MF types and epoch numbers) and the other one is studying the best models' results in order to understand the effects of each parameters on spray patterns for emulsified fuels.

The steps during simulation, namely generating results, are explained as followings. Primarily, the dataset is divided into two groups, the first is the training dataset with 80% of the all dataset including initial and end entries. The second one is the test dataset with the remaining 20% of all. All entries in these two datasets are selected randomly only leaving extreme values in the training dataset. The datasets are loaded into the ANFIS model in MATLAB with matrices called workspaces. Afterwards, the membership functions, rule numbers and rule types are selected in accordance with a variety of inputs. The optimum epoch number is then found the principle of that when epoch number is not adequate, the model becomes less accurate due to lack of neural networks in the system and when it is higher than required, it causes less accuracy again since it increases complicacy of neural networks which then diverges the results. All these arrangements are made with iteration and benefitting from previous studies on the ANFIS.

5.1. Remodelling the First Experimental Study

The study of Emberson et al. (2016) is evaluated firstly. The dataset from the figures belonging to that study is simulated in 17 different models shown below. The models are structured based on various input MF functions such as trimf, pimf and gaussmf, and the MF output type of "constant" and "linear" is tested to reach more accurate models. Then the epoch numbers are varied to find the best model option comparing the RMSE values of each and every model.

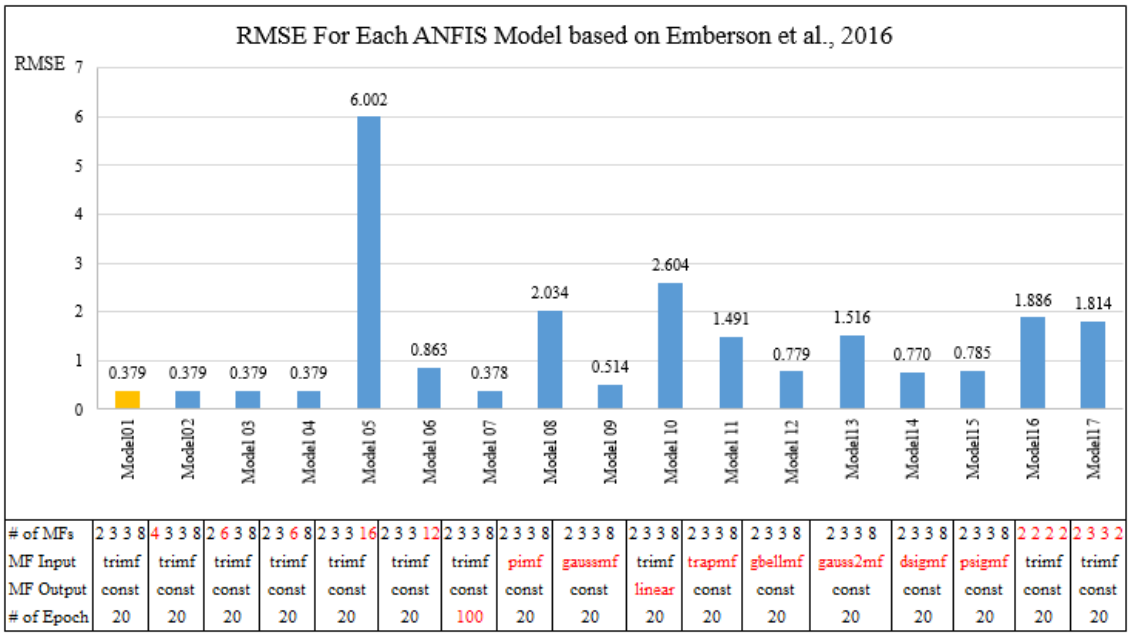

Figure 5.1. The RMSE of various ANFIS models from data of Emberson et al. (2016)

As seen from Figure 5.1, the Model 01 (amber bar in the figure) is found as the optimum one because it has one of the lowest RMSE value while its rule number of 96 and epoch number of 20 are not as much as the others which provides leaner transactions in the software which means less processing during running the simulation. Model 01 contains MF structure of 2-3-3-8, MF input of trimf and MF output of constant with 20 epoch number. The structure of the model produces 96 rules shown as blue layer in Figure 5.2 within the neural network model among 5 main layers.

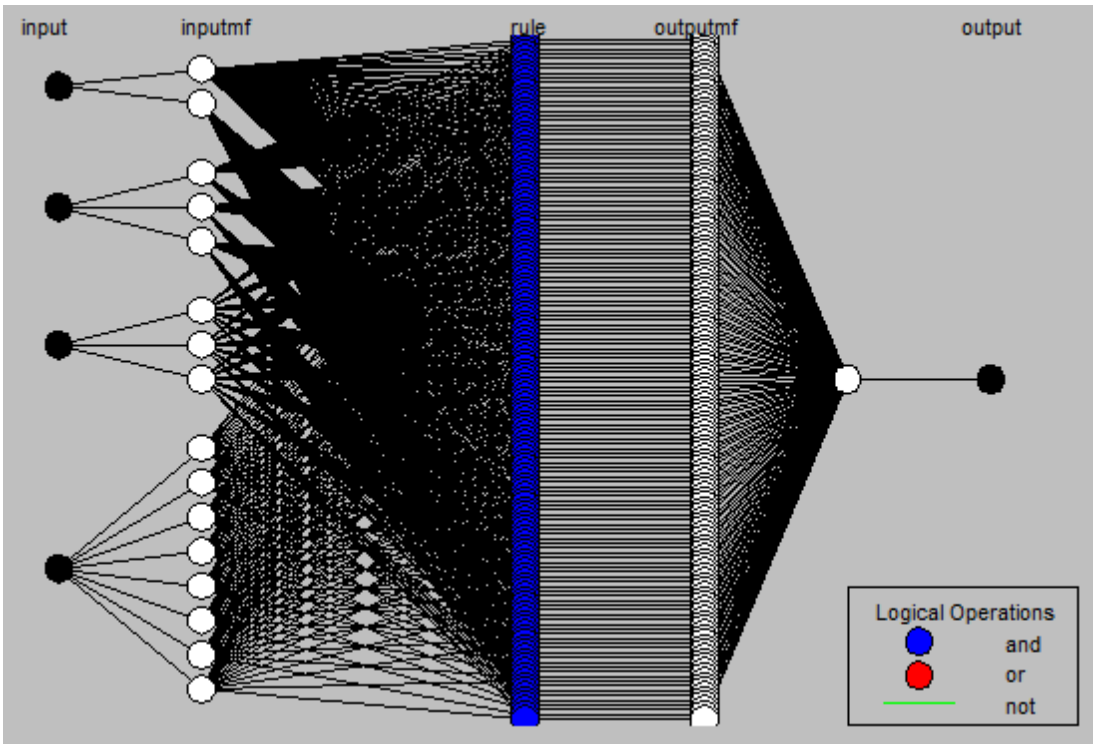

Figure 5.2. ANFIS Model Structure with neural networks and layers for Model01 (MF Structure: 2-3-3-8, Input MF: trimf, Epoch:20)

MATLAB provides a graph of the errors of the simulation results with respect to the given output results, which are experimental results from studies in our thesis. Figure 5.3 illustrates an example for this displaying testing data as blue dots and FIS outputs as red stars on top, and the overall RMSE of 0.37927 at the bottom. The RMSE value corresponds to a commendable accuracy of 98,4% in terms of test dataset.

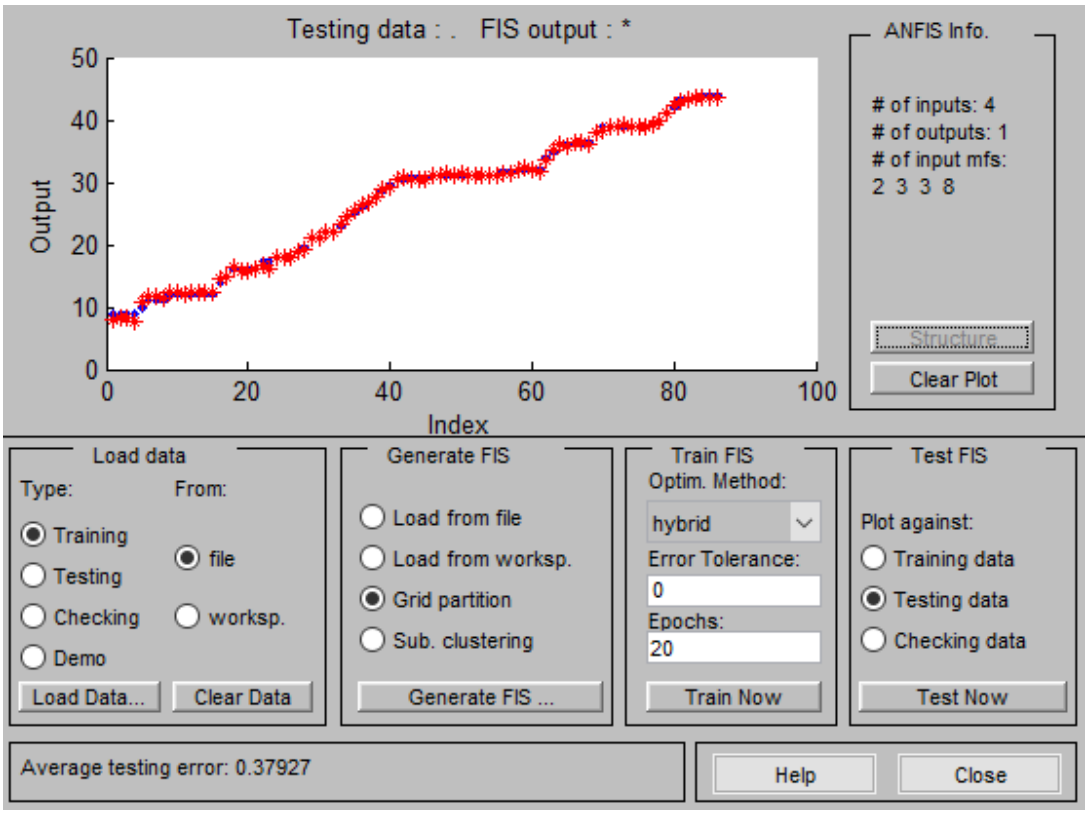

Figure 5.3. ANFIS Interface for Model 01 modelling with testing data as blue dot & FIS output as red star at the top with RMSE of 0.37927 at the bottom

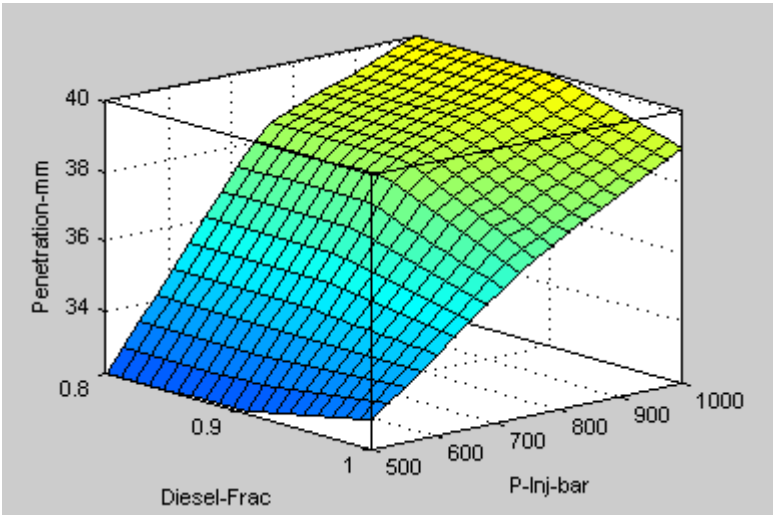

Figure 5.4. Spray penetration vs. diesel fraction at injection pressure where P_{amb} = 30 bar and t = 1000 µs

From Figure 5.4, the penetration values at 30 bar of ambient pressure and 1000 µs after SOI are shown with respect to injection pressure and diesel fractions not only with one to one inputs of the paper but also with interpolated values. The penetration is as

expected increasing with the increasing injection pressure. In terms of the water fractions, the neat diesel has a lower range of variety of penetration than the emulsion. As well as the values are very close in each diesel fraction for the emulsions including water more than 10%, the emulsion of 20% of water has the lowest and highest penetration at all with minimum and maximum injection pressure subsequently. Also it is apparent that the penetration up to the injection pressure of 750 bar increases more drastically than after the 750 bar.

It is also observed that addition of water slightly increases ultimate spray penetration value. The difference between 10% and 20% water addition is negligible at injection pressure of 1000 bar. The reason behind that water has higher volatility and less viscosity than diesel which causes higher displacement in the same injection conditions. Additionally, at lower injection pressure values, the emulsion decreases penetration since neat diesel has higher penetration value by around 3%.

5.2. Remodelling the Second Experimental Study

Following the same approach as the previous study, several ANFIS models based on Huo et al. (2014) were applied investigating firstly MF structure, namely rule numbers, from 1-1-2 (2 rules) to 4-6-16 (384 rules). It is observed that 2-3-4, 4-3-4 and 2-6-4 give the most accurate outputs as seen Figure 5.5 below. The “2-3-4” rules are selected to be utilized for further investigations since it requires lower processing during computation due to lower number of rules than others.

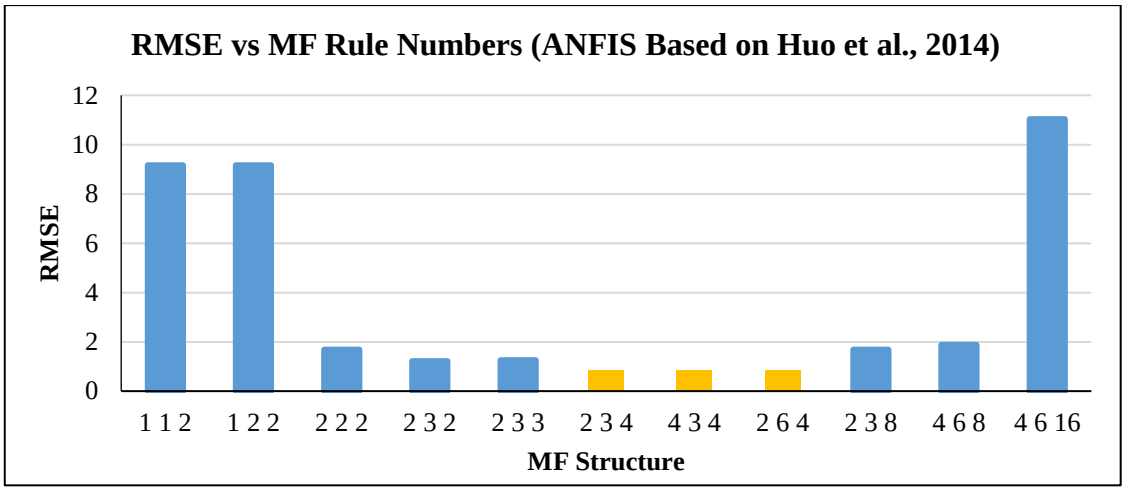

Figure 5.5. RMSE vs the MF structure in terms of rule numbers are firstly studied from 1-1-2 to 4-6-16 (number of 2 rules to 384 rules)

Secondly, the input and output types of each and every MF is studied and RMSE values are investigated. It is observed that input of "gaussmf" and output type of "linear" gives the best result as RMSE of 0.40056 while trimf-linear is as 7.5927 with highest RMSE in Figure 5.6.

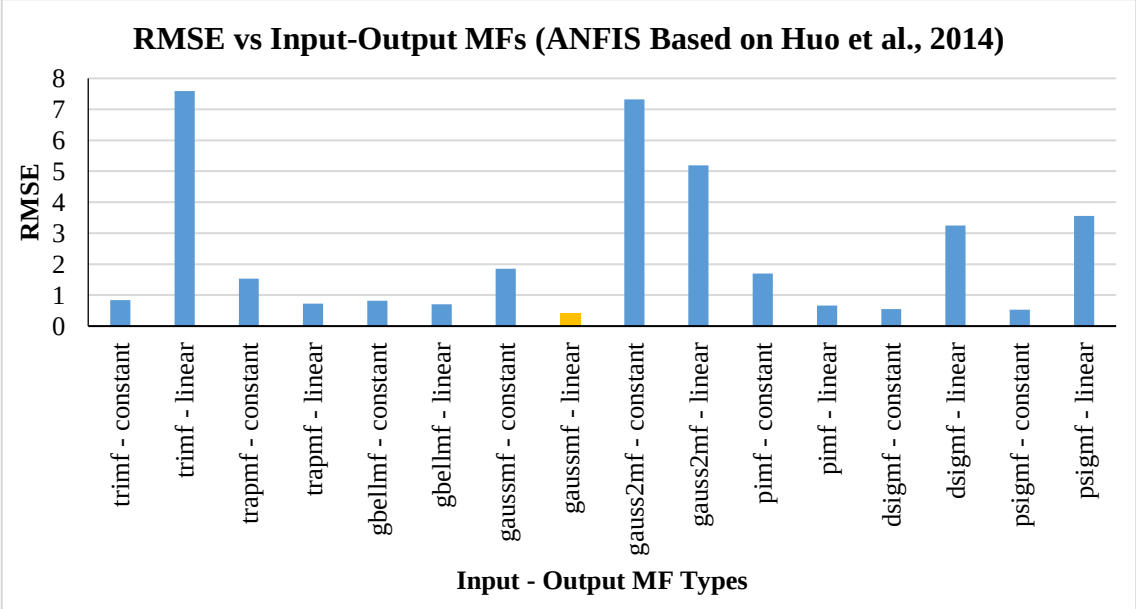

Figure 5.6. RMSE vs MF input function and output type

Then, the epoch numbers are investigated and it is found that the best result of ANFIS is obtained with 1 epoch number with RMSE of 0.39944 with the rule number of 2-3-4, input type of "gaussmf" and output type of linear. In Figure 5.7 below, it is

interestingly observed that the higher epoch numbers are giving the same RMSE of 0.40056 till the epoch number of 1000. In general, the training in every epoch tries to converge to the value of the model output to the target. However, it is observed here that the model creates the converged model in its first try.

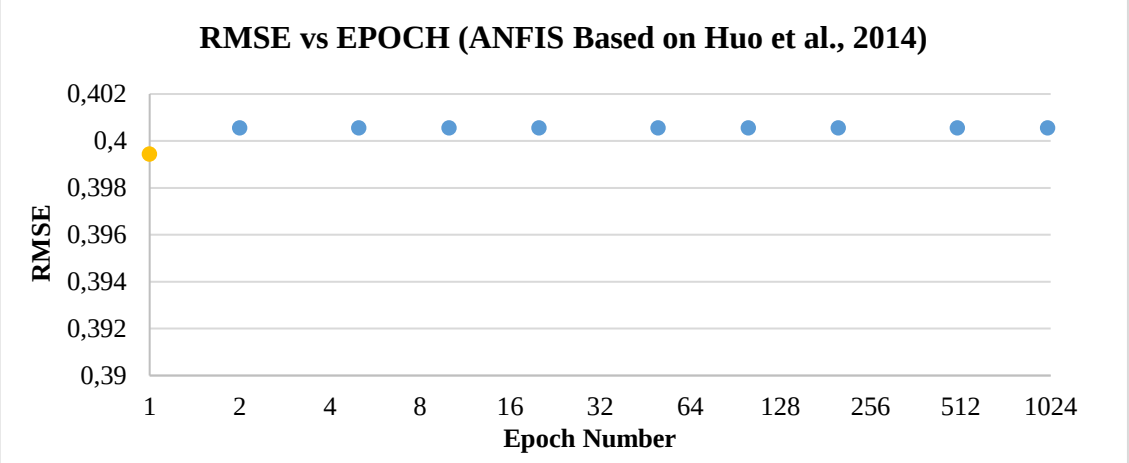

Figure 5.7. RMSE vs Epoch Numbers

In Figure 5.7 above, it is seen that in general, the training in every epoch tries to converge the value of the model output to better match the target.

After the construction of ANFIS model based on Huo et al. (2014) inputs and outputs the results of MATLAB are extracted. First the effects of diesel fraction between neat diesel and 20% water content with time over penetration are observed when ambient temperature is 800 K.

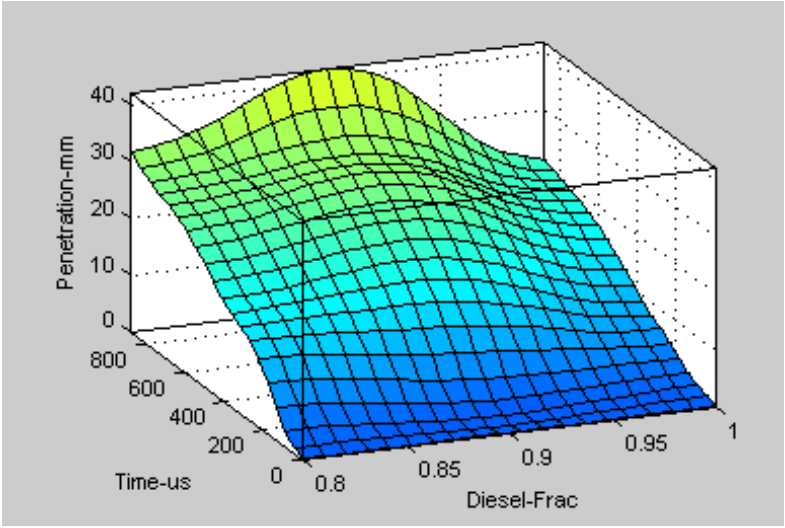

Figure 5.8. Penetration vs diesel fraction and time ASOI at T_{amb}=800 K

It is observed form Figure 5.8 that, the penetration is highest with 10% water content around 42 mm. Moreover, it is seen that the emulsions increase penetration where 20% water content has the penetration of around 32 mm while neat diesel has the penetration of 21 mm. The theoretical background of these circumstances is that diesel fraction has higher penetration with water content since the water has lower volatility than neat diesel.

From Figure 5.9, the effects of ambient temperature and diesel fraction over penetration are examined for the selected moments at 300 μs, 600 μs, and 880 μs. It is obviously seen that the maximum penetration value is increasing with increasing time. In earlier, the 20% water content and lowest ambient temperature of 527 °C has the highest penetration. After then the 10% water content reaches the maximum penetration with time. In Huo's study (2014), it is stated that due to the low volatility of the water under low ambient temperatures, emulsified diesel demonstrates longer penetration. Then at very high ambient temperatures like 1200 K, emulsified fuel performs similar liquid penetration length with neat diesel stating that the ambient temperature impact surpasses the physical properties of fuel such as viscosity, volatility and surface tension. Moreover, it is expressed that 10% water content are fattened at early stages of the spray evolution. However, spray pattern beginning fattened does point out more striking breakup through the process since the increase of water content may also cause to longer micro-explosion delay and so lower micro-explosion strength, which may interpret the reason of longer penetration for 10% water content regarding to 20% water content. Additionally, it is observed that the ambient temperature decreases penetration for all time in three surface plots below.

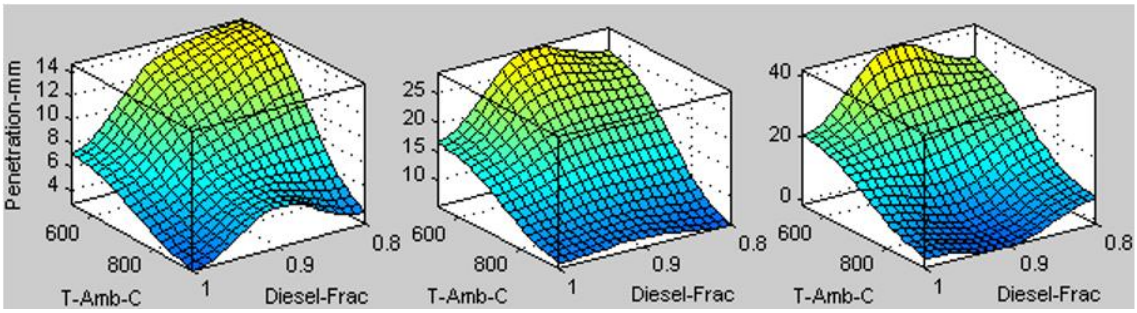

Figure 5.9. The effects of diesel fraction (from Neat Diesel to 80% Diesel+20% Water Emulsion) with Ambient Temperature when time = 300 μs, 600 μs and 880 μs subsequently

5.3. Study Based on Combined Data

The study based on the data combining the Huo's and Emberson's studies dataset is performed during this study. The Huo's study includes the effects of ambient temperature in addition to Emberson's analysis. By means of the ANFIS model the inputs and outputs of these two separate experiments are combined. Thereby the effects of ambient temperature are tried to be observed in the conditions of Emberson's works which was not available in the original study.

The training dataset is modelled with the program and the allocated testing data is then compared with actual experimental data. As it is seen from Figure 5.10 the model outputs are quite similar with actual experimental results except for 3 results at the latest part (in red stars). The input of these deviant outputs than transferred to training dataset form testing dataset to train a more accurate model.

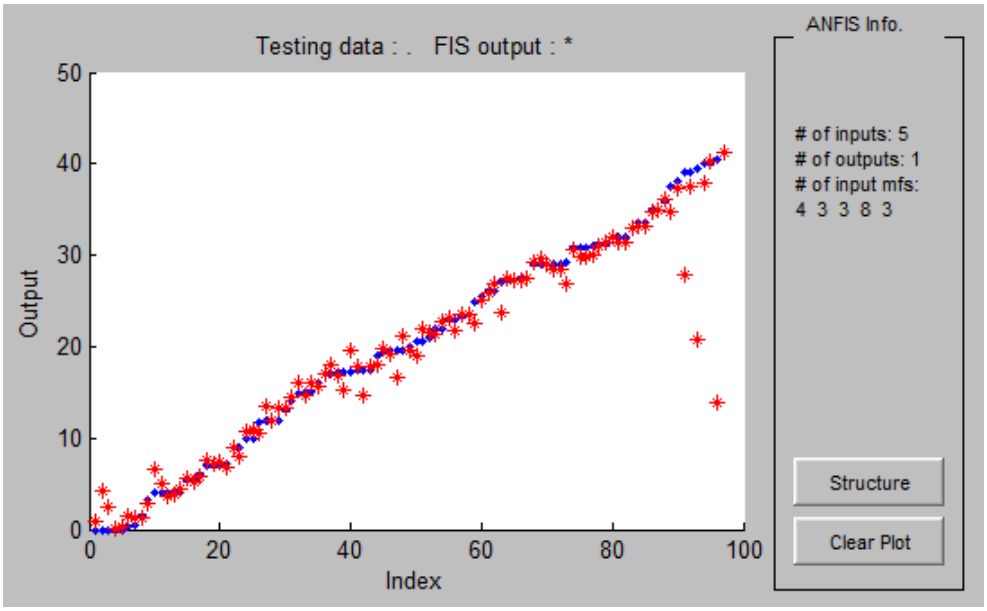

Figure 5.10. The comparison of ANFIS study with software model output (in red stars) and actual experimental outputs (in blue dots)

After arranging the training and test dataset in order to reach to most accurate results in terms of modelling, Figure 5.11 has been reached. The accuracy of the model is 98.4% with the RMSE of 0.96 which is quite satisfactory.

Figure 5.11. The comparison of ANFIS study with software model output (in red stars) and actual experimental outputs (in blue dots) after revisions of dataset

The simulation in Matlab is achieved with ANFIS model which has the trimf membership function with the total rule numbers of 864 in a structure of 4-3-3-8-3 benefitting from previous studies in previous subsections.

The figures below demonstrate the results including not only previous papers data but also interpolated data in the range of studies' dataset namely creating new results.

In Figure 5.12, it is clearly seen that the penetration is higher with lower ambient temperature. The figure is produced benefitting from two separate studies one of which is focused ambient temperature only at 300 K and the other one is at 800 K and 1200 K. At 1200 K, the penetration amount is lower and the duration is shorter since it reaches a quasisteady state promptly after initiation of injection. The higher ambient temperature conditions given, the higher evaporation and more violent dissolution of spray jet overcomed the impact of other properties such as volatility and surface tension. At 500 K, there is seen a drop-in penetration after 800 μs. The spray penetration prediction is shown in Figure 5.12. It can be seen that as the temperature increases the spray penetration decreases. The model is based on available data at 300 K, 800 K and 1200 K. The prediction data during the first 400 μs appears to be quite reliable. However, as the injection duration continues, the penetration values for the extrapolated conditions, namely 500 K and 700 K, appear to increase more rapidly than it should be expected. This could be due to the difference in injection duration input into the model. Whereas

for 300 K the injection duration input was 1200 μs, for the higher temperature conditions it was longer as the penetration dropped due to the start of combustion process, see (Huo et al., 2014). The problem the model is facing at this stage is that it is not only extrapolating data in terms of temperature but also in terms of injection duration. Thus, the error appears to be of higher magnitude. This would explain the sudden decrease of penetration for the 500 K case after 800 μs ASOI.

The conditions of two base studies are not totally same therefore the program tries to reach best predicted results that it can be concluded that the overall penetration value is lower in 500 K by compared with the lower temperature values.

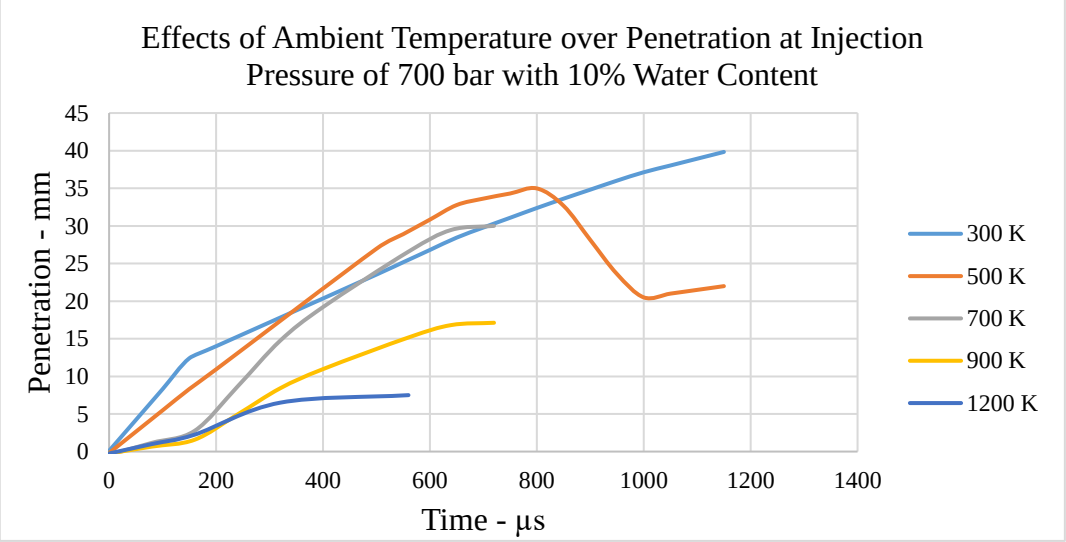

Figure 5.12. Effects of Ambient Temperature over Penetration at Injection Pressure of 700 bar with 10% Water Content

Figure 5.13 shows the spray penetration as a function of water content in diesel fuel for two ambient temperature conditions. It can be seen that at 300 K the addition of water has little effect on the liquid penetration. The lower volatility of water does not appear to increase penetration much because of the low ambient temperature. As temperature is increased, the emulsions spray penetration increases, since the lower water volatility has higher effect at higher temperatures. As the water content is increase the model shows an increase in spray penetration. This appears to be the case for lower temperature and the early stages of injection. However, for very high temperatures the ambient conditions overcome the volatility effects on the sprays. It appears that the model shows a shorter penetration for the 20% water content when compared with the 10% water

content at 900K. This is inherent from the experimental data imported from (Huo et al., 2014). They showed that at these medium-high temperatures the increase of water content to levels of about 20% provoked a deformation in the spray structure, making it wider and shorter.

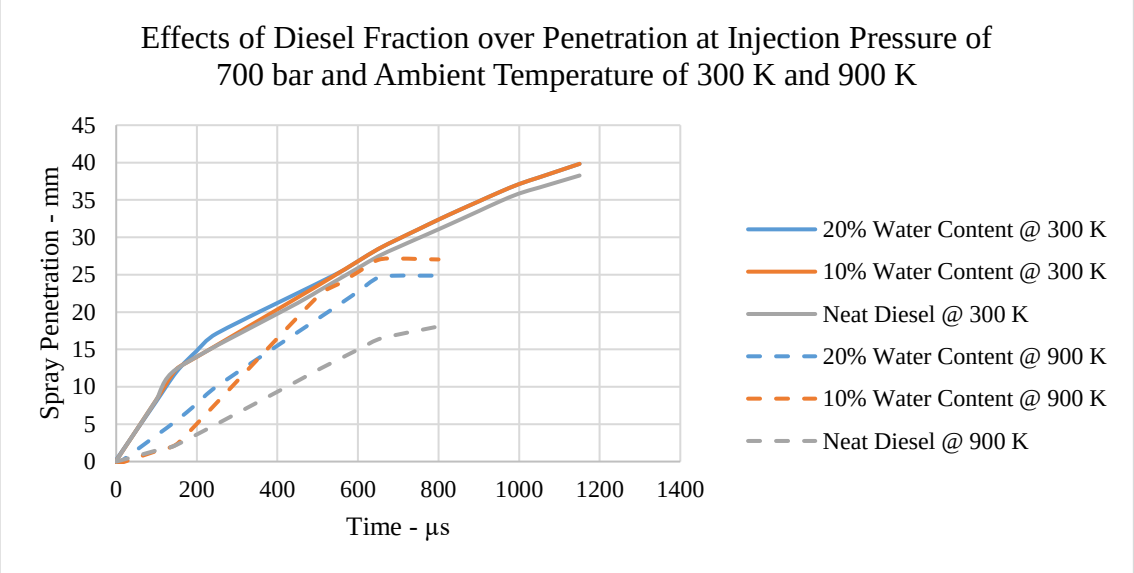

Figure 5.13. Effects of Diesel Fraction over Penetration at Injection Pressure of 700 bar and Ambient Temperature of 300 K and 900 K

CHAPTER 6

CONCLUSION

This study has investigated a numerical way of estimating the spray penetration value in a compression ignition engine using water emulsified diesel fuel as well as neat diesel. Our estimations are obtained using ANFIS tools of Matlab benefitting from two different studies from literature which are:

- "Optical characterization of Diesel and water emulsion fuel injection sprays using shawdography" by Emberson et al. (2016).
- "Study on the spray and combustion characteristics of water–emulsified diesel" by Huo et al. (2014).

The analysis of results indicates several important conclusions for the use of the software tool.

First, ANFIS models provide an accurate estimate of penetration as the forecasted values of models fit quite well to the actual data. Comparing to curve fitting or other mathematical tools, ANFIS shows some crucial advantages such as that ANFIS can generate different calculations depending on membership functions, rule numbers and epoch number while the other tools can only create one result per dataset. Additionally, ANFIS can tolerate more the deviated data points with its training capability while such data remarkably affect estimations in curve fitting.

Second, the membership functions of "trimf" and "gaussmf" outperforms the other membership functions during the study producing less RMSE. The rule number in accordance with variety of inputs also creates more accurate results.

Third, ANFIS models are quite robust to reach interpolated values of actual data. On the other hand, the extrapolated results of the ANFIS models are not satisfactory.

Finally, the most important lesson we get from our analysis is that ANFIS with true modelling structure can be useful to reach highly accurate results as well as generating outputs combining the datasets of different experiments relevantly without the need of repeating experiments.

The study above with ANFIS models has shown that the emulsion increases liquid penetration especially with 10% water in diesel emulsions likewise injection pressure.

Ambient temperature on the other hand decreases liquid penetration in general. With respect to the ambient temperature of 300 K, the liquid penetration is halved in 900 K and it reduces to its quarter in 1200 K.

For further study, the current studies having a larger number of data and range of data can be investigated for the comparison of spray behaviours in which data set may create more accurate results comparatively.

REFERENCES

Abani, N., & Reitz, R. (2007). Unsteady turbulent round jets and vortex motion. *Phys Fluids, 19:125102*, 1-13.

Abani, N., Kokjohn, S., Park, S. W., Bergin, M., Munnannur, A., Ning, W., . . . Reitz, R. D. (2008). An improved spray model for reducing numerical parameter dependencies in diesel engine CFD simulations. *SAE Paper, No: 2008–01-0970*.

Abu-Zaid, M. (2004). Performance of single cylinder, direct injection diesel engine using water fuel emulsions. *Energy Convers Manage, 45(5)*, 697–705.

Amsden, A. (1997). KIVA-3V, A Block-Structured KIVA program for Engines with Vertical or Canted Valves. *Los Alamos National Laboratory, LA-13313-MS*.

Armas, O., Ballesteros, R., Martos, F. J., & Agudelo, J. R. (2005). Characterization of light duty diesel engine pollutant emissions using water-emulsified fuel. *Fuel, 84*, 1011-1018.

Baneshi, M., Schaffie, M., Nezamabadi-pour, H., Behzadijo, M., & Rostami, M. (2015). Accurate Estimation of Petrophysical Indexes by RBF, ANFIS, and MLP Networks. *Energy Sources, Part A: Recovery, Utilization, and Environmental Effects, 37:17*, 1874-1882.

Barnaud, F., Schmelzle, P., & Schulz, P. (2000). AQUAZOLE ™ : An Original Emulsified Water-Diesel Fuel for Heavy-Duty Applications. *SAE 2000-01-1861*, 1-7.

Benajes, J., Payri, R., Bardi, M., & Martí-Aldaraví, P. (2013). Experimental characterization of diesel ignition and lift-off length using a single-hole ECN injector. *Appl. Therm. Eng.; 58*, 554-563.

Borman, G. L., & Ragland, K. W. (1998). *Combustion Engineering.* New York: McGraw-Hill.

Canakci, M., Ozsezen, A. N., Arcaklioglu, E., & Erdil, A. (2009). Prediction of performance and exhaust emissions of a diesel engine fueled with biodiesel produced from waste frying palm oil. *Expert Syst. Appl. 36*, 9268-9280.

Cay, Y. (2013). Prediction of a gasoline engine performance with artificial neural network. *Fuel 111*, 324–331.

Cay, Y., Korkmaz, I., Cicek, A., & Fuat, K. (2013). Prediction of engine performance and exhaust emissions for gasoline and. *Energy, 50*, 177-186.

Das, S. K., Kumar, A., Das, B., & Burnwal, A. P. (2013). On soft computing techniques in various areas. *Int J Inform Tech Comput Sci, 3*, 59-68.

Dec, J. E. (1997). A Conceptual Model of DI Diesel Combustion Based on Laser-Sheet Imaging. *SAE Technical Paper, 970873*.

Dent, J. (1971). A basis for the comparison of various experimental methods for studying spray penetration. *SAE Paper No. 710571*.

Desantes, J. M., Arregle, J., Lopez, J. J., & Cronhjort, A. (2006). Scaling laws for free turbulent gas jets and diesel-like sprays. *Atomization Spray 16, 4*, 443-474.

Desantes, J. M., Pastor, J. V., García-Oliver, J. M., & Brice, F. J. (2014). An experimental analysis on the evolution of the transient tip penetration in reacting diesel sprays. *Combust. Flame 161 (8),* 2137-2150.

Desantes, J. M., Pastor, J. V., García-Oliver, J. M., & Pastor, J. M. (2009). A 1D model for the description of mixing-controlled reacting diesel sprays. *Combustion and Flame 156, 1*, 234–249.

Desantes, J. M., Payri, R., Salvador, F. J., & Soare, V. (2015). Study of the influence of geometrical and injection parameters on diesel sprays characteristics in isothermal conditions. *SAE Paper No. 2005–01-0913*.

Emberson, D., Ihracska, B., Imran, S., & Diez, A. (2016). Optical characterization of Diesel and water emulsion fuel injection sprays using shadowgraphy. *Fuel 172*, 253-262.

Fahd, M., Wenming, Y., Lee, P. S., Chou, S. K., & Yap, C. (2013). Experimental investigation of the performance and emission characteristics of direct injection diesel engine by water emulsion diesel under varying engine load condition. *Appl Energy, 102(0),* 1042–9.

Fuchihata, M., Ida, T., & Mizutani, Y. (2003). Observation of microexplosions in spray flames of light oil-water emulsions (2nd report, influence of temporal and spatial resolution in high speed videography). *Trans Jpn Soc Mech Eng B 69*, 1503-1508.

Ganesan, P., Rajakarunakaran, S., Thirugnanasambandam, M., & Devaraj, D. (2015). Artificial neural network model to predict the diesel electric generator performance and exhaust emission. *Energy 83*, 115-124.

García-Oliver, J., Margot, X., Chávez, M., & Karlsson, A. (2011). A combined 1D3D–CFD approach for reducing mesh dependency in Diesel spray calculations. *Mathematical and Computer Modelling 54*, 1732–1737.

Garg, A. B., Diwan, P., & Saxena, M. (May de 2012). Artificial Neural Networks based Methodologies for Optimization of Engine Operations. *International Journal of Scientific & Engineering Research, 3*(5), 1-5.

Hay, N., & Jones, P. (1972). Comparison of the various correlations for spray penetration. *SAE Paper No. 720776.*

Hiroyasu, H., Kadota, T., & Arai, M. (1980). Supplementary Comments: Fuel Spray Characterization in Diesel Engines. in James N. Mattavi and Charles A. Amann (eds.), Combustion Modeling in Reciprocating Engines. *Plenum Press*, 369-408.

Hosoz, M., Ertunc, H. M., Karabektas, M., & Ergen, G. (2013). ANFIS modelling of the performance and emissions of a diesel engine using diesel fuel and biodiesel blends. *Appl. Therm. Eng. 60*, 24–32.

Huo, M., Lin, S., Liu, H., & Lee, C. F. (2014). Study on the spray and combustion characteristics of water–emulsified diesel. *Fuel 123*, 218-229.

Jang, J. (1993). ANFIS: Adaptive network-based fuzzy inference systems. *IEEE Transactions on Systems, Man, and Cybernetics 23*, 665-685.

Kadota, T., & Yamasaki, H. (2002). Recent advances in the combustion of water fuel emulsion. *Prog Energy Combust Sci, 28*, 385-404.

Kiani, M. K., Ghobadian, B., Tavakoli, T., Nikbakht, A. M., & Najafi, G. (2010). Application of artificial neural networks for the prediction of performance and exhaust emissions in SI engine using ethanol-gasoline blends. *Energy 35*, 65–69.

Kiplimo, R., Tomita, E., Kawahara, N., & Yokobe, S. (2012). Effects of spray impingement, injection parameters, and EGR on the combustion and emission characteristics of a PCCI diesel engine. *Appl. Therm. Eng. 37*, 165-175.

Lee, C. H., & Reitz, R. D. (2012). A comparative study on CFD simulation of spray penetration between gas jet and standard KIVA-3V spray model over a wide range of ambient gas densities. *J Mech Sci Technol, 26*(12), 4017–25.

Lee, C. H., & Reitz, R. D. (2013). CFD simulations of diesel spray tip penetration with multiple injections and with engine compression ratios up to 100:1. *Fuel - 111*, 289–297.

Lee, C. H., Wang, Y., & Reitz, R. D. (2011). CFD simulation of diesel sprays over a wide range of ambient gas densities using an improved gas jet spray model. *Atomization Spray 21 (7)*, 591–609.

Lee, S., Howlett, R., Crua, C., & Walters, S. (2007). Fuzzy logic and neuro-fuzzy modelling of diesel spray penetration: A comparative study . *Journal of Intelligent & Fuzzy Systems 18*, 43-56.

Lefebvre, A. H. (1989). *Atomization and Sprays.* London: Taylor and Francis.

Lif, A., & Holmberg, K. (2006). Water-in-diesel emulsions and related systems. *Adv Colloid Interface Sci, 123*, 231-239.

Lin, C. Y., & Lin, S. A. (2007). Effects of emulsification variables on fuel properties of two-phase and three-phase biodiesel emulsions. *Fuel, 86*, 210-217.

Lin, C., & Chen, L. (2008). Comparison of fuel properties and emission characteristics of two- and three-phase emulsions prepared by ultrasonically vibrating and mechanically homogenizing emulsification methods. *Fuel, 87*, 2154-2161.

Liu, B., Zhao, C., Zhang, F., Cui, T., & Su, J. (2013). Misfire detection of a turbocharged diesel engine by using artificial neural networks. *Applied Thermal Engineering, 55*, 26-32.

Liu, H., Lee, C., Ming, H., & Yao, M. (2011). Comparison of ethanol and butanol as additives in soybean biodiesel using a constant volume combustion chamber. *Energy Fuels, 25*, 1837-1846.

Maiboom, A., & Tauzia, X. (2011). NOx and PM emissions reduction on an automotive HSDI diesel engine with water-in-diesel emulsion and EGR: an experimental study. *Fuel, 90*, 3179-3192.

Mariani, F., Grimaldi, C., & Battistoni, M. (2014). Diesel engine NOx emissions control: An advanced method for the O2 evaluation in the intake flow. *Applied Energy 113*, 576-588.

Mathworks. (2016). *ANFIS*. Retrieved from http://www.mathworks.com/help/fuzzy/anfis.html

Mathworks. (2016). *ANN*. Retrieved from http://www.mathworks.com/help/nnet/gs/neural-networks-overview.html

Mathworks. (2016). *FUZZY*. Retrieved from http://www.mathworks.com/help/fuzzy/pimf.html

Mathworks. (2016). *GA*. Retrieved from http://www.mathworks.com/help/gads/what-is-the-genetic-algorithm.html

Mattiello, M., Cosmai, L., & Pistone, L. (1992). Experiment evidence for microexplosions in water/fuel oil emulsion flames inferred by laser light scattering. *Symp Combust 24*, 1573–8.

Mohan, B., Yang, W., & Chou, S. (2013). Fuel injection strategies for performance improvement and emissions reduction in compression ignition engines: a review. *Renew Sustain Energy Rev, 28(0)*, 664–76.

Mohan, B., Yang, W., & Chou, S. (2013). Fuel injection strategies for performance improvement and emissions reduction in compression ignition engines: a review. *Renew Sustain Energy Rev, 28(0)*, 664–76.

Musculus, M., & Kattke, K. (2009). Entrainment Waves in Diesel Jets. *SAE Technical Paper, 2009-01-1355*.

Musculus, M., Dec, E. J., Tree, R. D., Daly, D. D., Langer, D., & Ryam, W. T. (2003). Effects of water fuel emulsions on spray and combustion processes in a heavy-duty DI diesel engine. *SAE 2003-01-3146*.

Musculus, M., Miles, P., & Pickett, L. (2013). Conceptual models for partially premixed low-temperature diesel combustion. *Prog. Energy Combust. Sci. 39 (2)*, 246-283.

Naber, J. D., & Sieber, D. (1996). Effects of Gas Density and Vaporization on Penetration and Dispersion of Diesel Sprays. *SAE Technical Paper 960034, 960034*.

Nadeem, M., Rangkuti, C., Anuar, K., Haq, M. R., Tan, I. B., & Shah, S. S. (2006). Diesel engine performance and emission evaluation using emulsified fuels stabilized by conventional and gemini surfactants. *Fuel, 85*, 2111-2119.

Najafi, G., Ghobadian, B., Moosavian, A., Yusaf, T., Mamat, R., Kettner, M., & Azmi, W. H. (2016). SVM and ANFIS for prediction of performance and exhaust emissions of a SI engine with gasoline–ethanol blended fuels. *Applied Thermal Engineering, 95*, 186-203.

Namasivayam, A., Korakianitis, T., Crookes, R., Bob-Manuel, K., & Olsen, J. (2010). Biodiesel, emulsified biodiesel and dimethyl ether as pilot fuels for natural gas fuelled engines. *Appl Energy, 87(3)*, 769–78.

Palani, R., Nallusamy, N., & Pitchandi, K. (2015). Spray characteristics of diesel and derivatives in direct injection diesel engines with varying injection pressures. *Journal of Mechanical Science and Technology, 29 (10)*, 4465-4471.

Park, J. W., & K. Y. Huh, K. H. (2000). Experimental study on the combustion characteristics of emulsified diesel in a rapid compression and expansion machine. *Proc Inst Mech Eng Part D: J Automob Eng, 214 (5)*, 579-586.

Pastor, J. V., López, J. J., García, J. M., & Pastor, J. M. (2008). A 1D model for the description of mixing controlled inert diesel sprays. *Fuel 87*, 2871-2885.

Payri, F., Payri, R., Bardi, M., & Carreres, M. (2014). Engine combustion network: influence of the gas properties on the spray penetration and spreading angle. *Exp. Therm. Fluid Sci., 53,* 236-243.

Payri, R., García-Oliver, J. M., Xuan, T., & Bardi, M. (2015). A study on diesel spray tip penetration and radial expansion under reacting conditions. *Applied Thermal Engineering, 90,* 619-629.

Perini, F., Brakora, J. L., Reitz, R. D., & Cantore, G. (2012). Development of reduced and optimized reaction mechanisms based on genetic algorithms and element flux analysis. *Combust Flame 159,* 103-119.

Perini, F., Brakora, J. L., Reitz, R. D., & G., C. (2012). Development of reduced and optimized reaction mechanisms based on genetic algortihms and element flux analysis. *Combust Flame, 159,* 103-119.

Pickett, L., & Hoogterp, L. (2009). Fundamental spray and combustion measurements of JP-8 at diesel conditions. *SAE Int. J. Commer. Veh. 1 (1),* 108-118.

Postrioti, L., & Battistoni, M. (2010). Evaluation of Diesel Spray Momentum Flux in Transient Flow Conditions. *SAE International 2010-01-2244,* 1-21.

Qi, D., Chen, H., Matthews, R. D., & Bian, Y. Z. (2010). Combustion and emission characteristics of ethanol and biodiesel and water micro-emulsions used in a direct injection compression ignition engine. *Fuel, 89 (5),* 958-964.

Raul, O., Anna, L., Magnus, N., Sven, A., & Ingemar, D. (2010). Optical studies of spray development and combustion of water-in-diesel emulsion and micro emulsion fuels. *Fuel, 89,* 122-132.

Reddy, M., & Mohanta, D. (2007). A wavelet-neuro-fuzzy combined approach for digital relaying of transmission line faults. *Electr. Power Compon. Syst., 35*, 1385–1407.

Reitz, R., & Diwakar, R. (1986). Effect of drop breakup on fuel sprays. *SAE Paper No. 860469*.

Ringuest, J. L. (1992). Multi-Objective Optimization Behavioral and Computational Considerations. *Kluwer*.

Roisman, I., Araneo, L., & Tropea, C. (2007). Effect of ambient pressure on penetration of a diesel spray. *Int. J. Multiph. Flow, 33*(8), 904-920.

Roy, S., Banerjee, R., & Bose, K. P. (2014). Performance and exhaust emissions prediction of a CRDI assisted single cylinder diesel engine coupled with EGR using artificial neural network. *Applied Energy, 119,* 330-340.

Roy, S., Das, A. K., Bhadouria, V. S., Mallik, S. R., Banerjee, R., & Bose, P. K. (2015). Adaptive-neuro fuzzy inference system (ANFIS) based prediction of performance and emission parameters of a CRDI assisted diesel engine under CNG dual-fuel operation. *J. Nat. Gas Sci. Eng.*

Roy, S., Ghosh, A., Das, A. K., & Banerjee, R. (2015). Development and validation of a GEP model to predict the performance and exhaust emission parameters of a CRDI assisted single cylinder diesel engine coupled with EGR. *Appl. Energy 140*, 52-64.

Samadani, E., Shamekhi, A. H., Behroozi, M. H., & Chini, R. (2008). GA-Based Optimization of DI Diesel Engine Emission and Performance Using a Neural Network Model. *IEEE International (Annual) Conference on Instrumentation, Control and Information Technology, SICE2008.* Chofu, Japan.

Sayin, C., Ertunc, H. M., Hosoz, M., Kilicaslan, I., & Canakci, M. (2007). Performance and exhaust emissions of a gasoline engine using artificial neural network. *Appl. Therm. Eng. 27*, 46-54.

Sazhin, S. S., Feng, G., & Heikal, M. R. (2001). A model for fuel spray penetration. *Fuel 80, 15*, 2171-2180.

Shamekhi, A. H., Samadani, E., Behroozi, M. H., & Chini, R. (2009). A Method for Pre-Calibration of DI Diesel Engine Emissions and Performance Using Neural Network and Multi-Objective Genetic Algorithm. *Iran. J. Chem. Chem. Eng., 28*, 61-70.

Sharon, H., Jayaprakash, R., Sundaresan, A., & Karuppasamy, K. (2012). Biodiesel production and prediction of engine performance using SIMULINK model of trained neural network. *Fuel 99*, 197–203.

Siebers, D. (2009). *Flow and Combustion in Reciprocating Engines.* Springer.

Sinnamon, J. F., Lancaster, D. R., & Stiener, J. C. (1980). An experimental and analytical study of engine fuel spray trajectories. *SAE Paper No. 800135*.

Sisman-Yılmaz, N., Alpaslan, F., & Jain, L. (2004). ANFIS unfolded in time for multivariate time series forecasting. *Neurocomputing 61*, 139-168.

Song, K. H., & Lee, Y. J. (2000). Effects of emulsified fuels on soot evolution in an opticallyaccessible DI diesel engine. *SAE, 2000-01-2794*.

Sugeno, M., & Kang, G. (1988). Structure identification of fuzzy model. *Fuzzy Sets Syst., 28*, 15-33.

Taghavifar, H., Khalilarya, S., & Jafarmadar, S. (2014). Diesel engine spray characteristics prediction with hybridized artificial neural network optimized by genetic algorithm. *Energy, 71*, 656-664.

Takagi, T., & Sugeno, M. (1985). Fuzzy identification of systems and its applications to modeling and control. *IEEE transactions on systems, man, and cybernetics, vol. 15, no. 1*, 116-132.

Takasu, Y., Kaneko, S., Tominaga, H., Namura, Y., Inagaki, K., Ueda, M., & Tani, T. (2013). Universal diesel engine simulator (UniDES) 2nd report: Prediction of engine performance in transient driving cycle using one dimensional engine model. *SAE Paper No. 2013-01-0881*.

Tennison, P. J., Georjon, T. L., Farrell, P. V., & Reitz, R. D. (1998). An Experimental and numerical study of sprays from a common rail injection system for use in an HSDI Diesel engine. *SAE Paper No. 980810*.

Valdmanis, E., & Wurlfhorst, D. E. (1970). Effects of emulsified fuels and water induction on diesel combustion. *SAE 700736*.

Watanabe, H., & Okazaki, K. (2013). Visualization of secondary atomization in emulsified fuel spray flow by shadow imaging. *Proc Combust Inst 34*, 1651-1658.

Widodo, A., & Yang, B. (2011). Machine health prognostics using survival probability and support vector machine. *Expert Syst. Appl. 38*, 8430–8437.

Wu, D. Y., Sheng, H. Z., Zhang, H. C., & Wei, X. L. (2007). Study on micro explosions procedure of diesel/water/methanol emulsions droplet. *J Xi'an Jiaotong Univ 41*, 772-775.

Xu, M., Sun, Y. C., Cui, Y., Deng, K. Y., & Shi, L. (2016). One-Dimensional Model on Fuel Penetration in Diesel Sprays with Gas Flow. *International Journal of Automotive Technology, Vol:17*, 109-118.

Yetilmezsoy, K., Fingas, M., & Fieldhouse, B. (2011). An adaptive neuro-fuzzy approach for modeling of water-in-oil emulsion formation. *Colloids and Surfaces A: Physicochem. Eng. Aspects, 389*, 50– 62.

Yusaf, T. F., Buttsworth, D. R., Saleh, K. H., & Yousif, B. F. (2010). CNG-diesel engine performance and exhaust emission analysis with the aid of artificial neural network. *Appl. Energy 87*, 1661–1669.

Zadeh, L. A. (1994). Fuzzy logic, neural networks and soft computing. *Commun ACM, 37*, 77-84.